

Reconciling S_8 : Insights from Interacting Dark Sectors

Rahul Shah,^{*,1} Purba Mukherjee,^{*,†} and Supratik Pal^{*,§}

^{*}Physics and Applied Mathematics Unit, Indian Statistical Institute,
203 B.T. Road, Kolkata 700108, India

[†]Centre for Theoretical Physics, Jamia Millia Islamia, New Delhi 110025, India

[§]Technology Innovation Hub on Data Science, Big Data Analytics and Data Curation,
Indian Statistical Institute, 203 B.T. Road, Kolkata 700108, India

E-mail: rahul.shah.13.97@gmail.com, purba16@gmail.com, supratik@isical.ac.in

Abstract. We do a careful investigation of the prospects of dark energy (DE) interacting with cold dark matter (CDM) in alleviating the S_8 clustering tension. To this end, we consider various well-known parametrizations of the DE equation of state (EoS), and consider perturbations in both the dark sectors, along with an interaction term. Moreover, we perform a separate study for the phantom and non-phantom regimes. Using CMB, BAO and SNIa datasets, the constraints on the model parameters for each case have been obtained and a generic reduction in the $H_0 - \sigma_{8,0}$ correlation has been observed, both for constant and dynamical DE EoS. This reduction, coupled with a significant negative correlation between the interaction term and $\sigma_{8,0}$, contributes to easing the clustering tension by lowering $\sigma_{8,0}$ to somewhere in between the early CMB and late-time clustering measurements for the phantom regime, for almost all the models under consideration. In addition, this is achieved without exacerbating the Hubble tension. In this regard, the CPL and JBP models perform the best in relaxing the S_8 tension to $< 1\sigma$. However, for the non-phantom regime the $\sigma_{8,0}$ tension tends to have worsened, which reassures the merits of phantom dark energy from latest data. We further do an investigation of the role of RSD datasets and find an overall reduction in tension, with a value of $\sigma_{8,0}$ relatively closer to the CMB value. We finally check if further extensions of this scenario, like the inclusion of the sound speed of dark energy and warm dark matter interacting with DE, can have some effects.

¹Corresponding author

Contents

1	Introduction	1
2	Interacting two fluid setup with CDM and DE	3
3	DE models and datasets used	5
4	Parameter estimation using MCMC	6
4.1	Non-phantom regime for DE	7
4.2	Phantom regime for DE	10
4.3	Comparison and interpretation	13
4.4	Any effect of keeping c_s^2 free?	14
5	Possible role of $f\sigma_8$ RSD data	16
6	DE interacting with warm DM	19
7	Conclusions	21

1 Introduction

The Λ CDM cosmological model, which assumes dark energy (DE) as a cosmological constant (Λ) and non-relativistic “cold” dark matter (CDM) as the primary constituents of the Universe, has provided valuable insights into various astrophysical and cosmological phenomena. However, recent inconsistencies arising from precise measurements of the model parameters, from different scales of observations, have raised questions regarding its effectiveness. Chief among these concerns is the 5σ Hubble tension [1–3], which has garnered significant attention in the scientific community, leading to numerous proposed explanations and alternative theoretical models [4–7]. However, a different, yet closely related tension exists in the measurements of the matter clustering strength within the Universe, as quantified by the $\sigma_{8,0}$ or $S_8 = \sigma_{8,0}\sqrt{\Omega_{m0}/0.3}$ parameter [8]. A discrepancy of $\sim 3\sigma$ exists between the values derived from cosmic microwave background (CMB) data from Planck 2018 [9] ($S_8 = 0.832 \pm 0.013/\sigma_{8,0} = 0.8111 \pm 0.0060$) and those inferred from observations at lower redshifts, *viz.* CFHTLenS [10] ($S_8 = 0.732^{+0.029}_{-0.031}$); KiDS-450 [11] ($S_8 = 0.745 \pm 0.039$), which when combined with 2dFLenS [12] gives $S_8 = 0.742 \pm 0.035$; KV450 [13] ($S_8 = 0.737^{+0.040}_{-0.036}$), on adding BOSS [14] gives $S_8 = 0.728 \pm 0.026$. DES-Y1 [15] obtains $S_8 = 0.782 \pm 0.027$, and in combination with KV450 [16] one gets $S_8 = 0.755^{+0.019}_{-0.021}$. KiDS-1000 [17] alone gives $S_8 = 0.759^{+0.024}_{-0.021}$, and KiDS-1000+BOSS+2dFLenS [18] finds $S_8 = 0.766^{+0.020}_{-0.014}$. DES-Y3 [19] finds $S_8 = 0.759^{+0.025}_{-0.023}$. However, at the same time, a few late-time probes give constraints closer to the early-time measurements, such as those from KiDS-450+GAMA [20] ($S_8 = 0.800^{+0.029}_{-0.027}$) and HSC SSP [21] ($S_8 = 0.804^{+0.032}_{-0.029}$).

Although the Λ CDM model more or less fits either set of data, observations at lower redshifts, in general, inarguably suggest a reduced level of structure formation resulting from the discrepancy in the inferred values of S_8 . Since the status of the clustering tension is less apparent than that of the Hubble tension, investigations into this aspect are significantly

overshadowed by studies on the latter. However, that there exists a strong positive correlation between H_0 and $\sigma_{8,0}$ has been pointed out earlier by couple of papers (see, for example, [22]). Treatments to alleviate one of these tensions often exacerbate the other, highlighting the need for a joint approach to address both consistently. The $\sigma_{8,0}$ parameter is particularly sensitive to cosmological dynamics at the perturbative level, which is more complex to consider both theoretically and observationally compared to the background evolution dependent H_0 . Herein lies the primary challenge in today’s precision cosmology - to simultaneously address both tensions, operating at different levels of observation, or at the very least, to address one without compromising the other.

There have been some level of efforts to alleviate the clustering tension (see [6, 8]). In this study, we aim to reassess this tension within the framework of interacting dark energy dark matter (iDMDE) models, which entails an exchange of energy between the dark sectors. Initially proposed to solve the coincidence problem in cosmology [23], these models have lately attracted a lot of attention in addressing the Hubble tension [7, 22, 24–47]. Of late they have been explored in the context of the clustering tension as well. For example, [29, 48] consider an iDMDE setup for Λ CDM, imposing hard bounds on the equation of state (EoS) parameter to avoid instabilities in the perturbations (also see [49]). In [22], an iDMDE treatment with perturbations is done by absorbing the interaction in terms of effective parameters, considering a CPL [50] parametrization of the effective EoS of DE. As a result, the correlation between the interaction term with other parameters is not evident. Refs. [44–46] consider interactions, but within the Λ CDM framework only, with no perturbations in the DE sector. Ref. [51] considers various forms of the interaction term and obtains constraints on the clustering parameter by keeping the EoS of DE free, but constant, *i.e.* an interacting w CDM setup. Similar efforts along these directions were carried out in [52–55] for different forms of the interaction term or alternative DE models. Usually, an interacting setup is characterised primarily by the coupling term, which governs the magnitude and direction of energy-momentum transfer. However, consensus regarding the precise form of this interaction remains elusive due to the inherently “dark” nature of the involved components, which hinders a well-founded first-principles field-theoretic formulation.

In this study, we aim to revisit and expand upon the existing literature by doing a systematic case-by-case analysis focussing on the clustering tension, albeit with the latest compilation of datasets, thus improving upon some of the existing studies which have since become outdated. Here, we utilise a combination of the latest CMB data from Planck 2018 [9], baryon acoustic oscillations (BAO) data and type-Ia supernovae (SNIa) observations from the Pantheon [56] compilation. We begin by considering an interaction term proportional to the DE density, a framework that has exhibited some promise in addressing cosmological tensions [26–29, 57, 58]. Unlike some of the previous approaches using effective parameters, we adopt a generic prescription and explore this model under different parametrizations of the DE EoS. This exercise can in turn help us explore whether these extensions to Λ can alleviate tensions in the presence of interactions. Nevertheless, we keep the provision open so that both DM and DE can take part in clustering, by considering generic first order cosmological perturbations in both the DM and DE sectors, thereby carefully accounting for the effect of the interactions and the nature of DE on the perturbative level.

It is crucial to highlight that, when perturbation in DE is considered, the velocity perturbation equation for the DE sector blows up if the EoS reaches exactly $w = -1$ at any point during cosmic evolution. Thus, for the dynamical dark energy (DDE) models, it is imperative to prevent phantom-crossing to avoid instabilities in the perturbation equations. Hence we

deal with the phantom and non-phantom regimes separately as they are entirely motivated by fundamentally distinct physics. This is the only restriction we impose in our analysis, thereby refraining from imposing any additional hard bounds on the interaction parameter or any other parameter, as has been commonly done in the past to avoid theoretical instabilities due to interactions. We keep the interaction parameter entirely free to explicitly examine if such instabilities arise in light of current datasets, hence enabling generic conclusions. We find that the presence of interactions for a phantom EoS of DE helps relax the $\sigma_{8,0}$ tension, without exacerbating the H_0 tension. However, a non-phantom case worsens the situation and hence is not favoured by latest datasets. We also see a generic reduction, and in some cases, a complete elimination of the $H_0 - \sigma_{8,0}$ correlation for the constant/dynamical dark energy (C/DDE) parametrizations. This allows for reduction of the $\sigma_{8,0}$ tension without significant changes in H_0 .

Since the $\sigma_{8,0}$ parameter is under focus, we further investigate the effect of incorporating the $f\sigma_8$ measurements from redshift space distortions (RSD) [59] observations in addition to the aforementioned combination of datasets. We find noticeably tighter constraints on certain parameters, including $\sigma_{8,0}$, which take relatively higher values compared to non-inclusion of RSD data. Although there still is an overall reduction in the clustering tension, the extent of it is reduced.

Moreover, the role of DE clustering, however small, can be revealed in the context of tensions, providing valuable insights into the behaviour of DE at small scales [60–64]. Therefore, attempts were made to constrain the DE sound speed c_s^2 by keeping it as a free parameter in our analyses. We found that c_s^2 remains almost unconstrained with current datasets, and hence has little effect on other parameters of interest. As a demonstrative case, we show how the overall constraints are affected if it is kept as a free parameter for w CDM. Moreover, as a minimal extension to the above scenarios, we investigate the role of a “non-cold” DM sector, parametrized via some non-zero but constant dark matter EoS, described by an extra free parameter w_{DM} .

We place particular attention to the $\sigma_{8,0}/S_8$ tension with our goal being to examine not only the effect of interactions within the dark sector but also the impact of DE perturbations and different parametrizations of C/DDE explicitly. In section 2, we provide a brief outline regarding the theoretical framework of the interacting dark sector. section 3 introduces various parametrizations of the EoS of DE in the interacting scenario considered in this work, along with an outline of the datasets employed for this study. Our results and analysis are presented in section 4. In Section 5 we study the effects on adding RSD data to the analysis. Section 6 explores the prospects of warm dark matter (WDM) in some of the interacting scenarios to gain an understanding of the role of the nature of dark matter (DM) in this context. Finally, we make some concluding remarks in section 7.

2 Interacting two fluid setup with CDM and DE

Understanding the interaction within the dark sector poses a significant challenge due to the lack of a fundamental understanding of each component, unlike the situation in the standard model of particle physics. However, a practical approach followed is to consider both DE and DM as ideal fluids, having a transfer of energy or momentum between both sectors. This perspective circumvents the need for a Lagrangian description of the system to gain cosmological insights. For a non-zero interaction between the two dark sectors, the energy-

momentum tensors of DE and DM are not independently conserved, rather,

$$\nabla_{\mu} T_{(k)}^{\mu\nu} = \mathcal{Q}_{(k)}^{\nu} \quad (2.1)$$

is satisfied, where the index k is “de” for DE and “dm” for DM, with $\mathcal{Q}_{(k)}^{\nu}$ quantifying the energy-momentum flux between them. Further, the Bianchi identity dictates the overall conservation of the energy-momentum tensor, and hence $\mathcal{Q}_{\text{de}}^{\nu} = -\mathcal{Q}_{\text{dm}}^{\nu}$. In this work, we consider only energy transfers to be possible ($\mathcal{Q}_{\text{de}}^0 = -\mathcal{Q}_{\text{dm}}^0 = \mathcal{Q}$), with no momentum transfer, implying $\mathcal{Q}_{(k)}^i = 0$.

Assuming DM to be cold, *i.e.* non-relativistic (CDM), we have the continuity equations,

$$\dot{\rho}_{\text{dm}} + 3\mathcal{H}\rho_{\text{dm}} = a^2 \mathcal{Q}_{\text{dm}}^0 = a\mathcal{Q}, \quad (2.2)$$

$$\dot{\rho}_{\text{de}} + 3\mathcal{H}(1+w)\rho_{\text{de}} = a^2 \mathcal{Q}_{\text{de}}^0 = -a\mathcal{Q}, \quad (2.3)$$

where an overhead dot represents derivative with respect to conformal time, $\mathcal{H} = aH$ is the conformal Hubble parameter, $w \equiv w(a)$ is the EoS of DE, and \mathcal{Q} is the rate of transfer of energy density, with $\mathcal{Q} > 0$ implying an energy transfer from DE to DM (as a solution to the coincidence problem [65]), and vice versa.

We assume the form of the interaction to be,

$$\mathcal{Q} = HQ\rho_{\text{de}}, \quad (2.4)$$

where Q is the coupling constant. The analytical solutions to the continuity equations above are then,

$$\rho_{\text{dm}} = \rho_{\text{dm},0} a^{-3} + \rho_{\text{de},0} a^{-3} Q \int_1^a \frac{a'^2 e^{\xi(a')}}{a'^Q} da', \quad (2.5)$$

$$\rho_{\text{de}} = \rho_{\text{de},0} \frac{e^{\xi(a)}}{a^Q}, \quad (2.6)$$

where $\xi(a) = \int_a^1 \frac{3[1+w(a')]}{a'} da'$.

The linear order perturbation equations for DM and DE in the synchronous gauge are given as [26, 66–69],

$$\dot{\delta}_{\text{dm}} = -\theta_{\text{dm}} - \frac{\dot{h}}{2} + \mathcal{H}Q \frac{\rho_{\text{de}}}{\rho_{\text{dm}}} (\delta_{\text{de}} - \delta_{\text{dm}}) + Q \frac{\rho_{\text{de}}}{\rho_{\text{dm}}} \left(\frac{kv_T}{3} + \frac{\dot{h}}{6} \right), \quad (2.7)$$

$$\dot{\theta}_{\text{dm}} = -\mathcal{H}\theta_{\text{dm}} \left(1 + Q \frac{\rho_{\text{de}}}{\rho_{\text{dm}}} \right), \quad (2.8)$$

$$\begin{aligned} \dot{\delta}_{\text{de}} = & -(1+w) \left(\theta_{\text{de}} + \frac{\dot{h}}{2} \right) - \frac{3\mathcal{H}\theta_{\text{de}}}{k^2} \dot{w} - Q \left(\frac{kv_T}{3} + \frac{\dot{h}}{6} \right) \\ & - 3\mathcal{H}(c_s^2 - w) \left[\delta_{\text{de}} + \{3(1+w) + Q\} \frac{\mathcal{H}\theta_{\text{de}}}{k^2} \right], \end{aligned} \quad (2.9)$$

$$\dot{\theta}_{\text{de}} = -\mathcal{H} \left(1 - 3c_s^2 \right) \theta_{\text{de}} + \frac{Q\mathcal{H}\theta_{\text{de}}}{1+w} (1 + c_s^2) + \frac{k^2 c_s^2}{1+w} \delta_{\text{de}}, \quad (2.10)$$

where δ_{dm} and δ_{de} denote the density contrasts, θ_{dm} and θ_{de} the velocity perturbations, and ρ_{dm} and ρ_{de} the densities, of DM and DE respectively. The DE adiabatic sound speed is set to the EoS of DE (w), c_s^2 is the sound speed of DE and v_T is the centre of mass velocity for the total fluid defined as, $(1 + w_T)v_T = \sum_a (1 + w_a)\Omega_a v_a$. The extra terms in the density contrast equations are due to the perturbation of the Hubble rate (δH) [26].

3 DE models and datasets used

In this study, we characterise DM as non-relativistic (CDM). We explore interacting scenarios by employing several well-established parametrizations of the EoS of DE. Perturbations are incorporated into both dark sectors to enable insights into the combined influences of interaction and perturbations. The diverse parametrizations of the DE EoS under examination are henceforth referred to as different models,

- We include an interacting Λ CDM as the benchmark model in our study, where the DE sector is characterised by a constant EoS $w = -1$, and, obviously, it does not take part in perturbations. We have included this in our analysis only to compare the performances of the alternative models against this baseline.
- Interacting w CDM is a minimal extension of Λ CDM where the DE EoS w is kept as a constant (not redshift-evolving) but otherwise free parameter, *i.e.* $w(a) = w_0$.
- The CPL parametrization of DE [50, 70], which is the most widely used two-parameter extension to Λ CDM has a redshift-dependent DE EoS given by,

$$w(a) = w_0 + w_a (1 - a) . \quad (3.1)$$

The present value of the EoS is given by w_0 , while it remains bounded by $w_0 + w_a$ in the far past. Its simple form and its ability to parametrize a wide range of theoretical DE models render it a particularly appealing choice.

- The JBP parametrization [71], another well-discussed DE parametrization that proposes the following form for the DE EoS,

$$w(a) = w_0 + w_a a (1 - a) . \quad (3.2)$$

- The modified emergent dark energy (MEDE) model is a simple generalisation of the phenomenological emergent dark energy (PEDE) model [72], obtained by including one additional degree of freedom α . Here the DE EoS takes the form [73],

$$w(a) = -1 - \frac{\alpha}{3 \ln 10} [1 - \tanh(\alpha \log_{10} a)] . \quad (3.3)$$

If $\alpha = 0$, the model reduces to the Λ CDM scenario, while for $\alpha = 1$ the PEDE model is recovered. In the present work, we re-parametrize α as $w_0 = -1 - \frac{\alpha}{3 \ln 10}$.

The following datasets are utilised in our analysis:

- **CMB**: Cosmic microwave background temperature and polarization angular power spectra, and CMB lensing of Planck 2018 *TTTEEE+low l+low E+lensing* [9, 74, 75].
- **BAO**: Baryon acoustic oscillations measurements by 6dFGS [76], SDSS MGS [77], and BOSS DR12 [78] (as used in the Planck 2018 analysis [9]).
- **SNIa**: Luminosity distance data of 1048 SNIa from the Pantheon compilation [56].

Parameter	Prior
$\Omega_b h^2$	[0.005, 0.1]
$\Omega_c h^2$	[0.01, 0.99]
$100\theta_s$	[0.5, 10]
$\ln(10^{10} A_s)$	[1, 5]
n_s	[0.5, 1.5]
τ	[0, 0.9]
Q	[-2, 2]
w_0	[-1, 0] in non-phantom regime
w_0	[-3, -1] in phantom regime
w_a	[-2, 2]
c_s^2	[0, 2]

Table 1: Priors used for obtaining constraints on the cosmological parameters of interest.

As argued in [79], we deliberately leave SH0ES [80] data out of this analysis in order to do an honest comparison of the H_0 values as obtained from the above datasets against the SH0ES value, so as to give a proper estimation of the Hubble tension (summarised in Table 4).

We implement the models under consideration into the Boltzmann solver code `CLASS`¹ [81, 82], building upon the publicly available modified versions by [26, 27], by employing Romberg integration methods for evaluating certain otherwise intractable integrals involving the dynamical EoS of DE. We also properly take into account the effect of the C/DDE parametrizations on the computation of the growth factor [83]. Constraints are obtained on the model parameters using `MontePython`² [84, 85], with the priors considered for the Markov chain Monte Carlo (MCMC) analyses as given in Table 1, by ensuring strict non-phantom and phantom bounds for the DE EoS parameters. The corresponding contour plots were generated using `GetDist`³ [86].

4 Parameter estimation using MCMC

Let us now present the results of our MCMC analyses on a case-by-case basis, with separate discussions on the phantom and non-phantom regimes for the DE sector. Such a treatment is justified due to various reasons. Firstly, the presence of a “doom factor” $[1/(1+w)]$ in the perturbation equations causes them to become singular if the EoS of the DE model undergoes phantom-crossing (at $w = -1$) at any point of cosmic evolution. Secondly, the inherently distinct nature of DE in the two regimes about the phantom divide line $w = -1$ necessitates a careful examination of each sector independently. Crossing the phantom divide line has two cosmological implications - either the DE consists of multiple components with at least one non-canonical phantom component, or general relativity needs to be extended to a more general theory on cosmological scales [87–89]. Moreover, when subjected to observational data, the two regimes exhibit distinct qualitative constraints on other cosmological parameters (see, *e.g.* [1, 2, 22]). These differences underscore the importance of treating them separately to ensure a robust theoretical framework for reliable and accurate interpretations of observational data.

¹https://github.com/lesgourg/class_public

²https://github.com/brinckmann/montepython_public

³<https://github.com/cmbant/getdist>

Note: Throughout the paper, we fix the sound speed of DE as $c_s^2 = 1$, except when it is explicitly mentioned to be varying (Sec. 4.4). Besides, whenever we refer to any model by its parametrization, the full effect of interactions is considered, unless $Q = 0$ is explicitly mentioned.

4.1 Non-phantom regime for DE

Table 2 shows the constraints on the interacting models considered in the non-phantom regime. The full triangle plots are in Fig. 1.

Parameters	Λ CDM	w CDM	MEDE	CPL	JBP
$\Omega_b h^2$	0.02241 ± 0.00014	0.02241 ± 0.00014	0.02242 ± 0.00015	0.02242 ± 0.00014	0.02239 ± 0.00014
$\Omega_c h^2$	$0.111^{+0.010}_{-0.0089}$	$0.079^{+0.034}_{-0.017}$	$0.079^{+0.039}_{-0.018}$	$0.067^{+0.033}_{-0.023}$	$0.099^{+0.038}_{-0.026}$
$100\theta_s$	1.04192 ± 0.00029	1.04192 ± 0.00029	1.04194 ± 0.00030	1.04192 ± 0.00029	1.04190 ± 0.00029
$\ln(10^{10} A_s)$	3.046 ± 0.015	3.046 ± 0.014	3.046 ± 0.015	3.047 ± 0.015	3.043 ± 0.015
n_s	0.9666 ± 0.0039	0.9669 ± 0.0039	0.9669 ± 0.0039	0.9671 ± 0.0039	0.9660 ± 0.0039
τ	0.0549 ± 0.0075	0.0551 ± 0.0074	$0.0551^{+0.0068}_{-0.0077}$	0.0555 ± 0.0077	0.0536 ± 0.0075
Q	-0.075 ± 0.092	$-0.33^{+0.25}_{-0.16}$	$-0.32^{+0.31}_{-0.15}$	-0.41 ± 0.19	-0.16 ± 0.27
w_0	-	$-0.911^{+0.033}_{-0.084}$	$-0.892^{+0.045}_{-0.11}$	$-0.882^{+0.050}_{-0.10}$	$-0.864^{+0.046}_{-0.13}$
w_a	-	-	-	$0.004^{+0.11}_{-0.13}$	-0.69 ± 0.55
H_0	68.32 ± 0.80	68.23 ± 0.82	68.10 ± 0.83	68.20 ± 0.88	68.23 ± 0.81
Ω_{m0}	0.288 ± 0.027	$0.219^{+0.075}_{-0.042}$	$0.221^{+0.089}_{-0.044}$	$0.195^{+0.070}_{-0.056}$	$0.263^{+0.083}_{-0.057}$
$\sigma_{8,0}$	$0.869^{+0.054}_{-0.082}$	$1.233^{+0.039}_{-0.43}$	$1.249^{+0.048}_{-0.47}$	$1.30^{+0.12}_{-0.55}$	$1.036^{+0.060}_{-0.35}$
S_8	$0.845^{+0.033}_{-0.028}$	$0.932^{+0.181}_{-0.074}$	$0.931^{+0.226}_{-0.085}$	$0.989^{+0.223}_{-0.102}$	$0.875^{+0.146}_{-0.072}$
χ^2_{min}	3811	3812	3812	3814	3811
$-\ln \mathcal{L}_{min}$	1905.64	1906.22	1906.02	1907.07	1905.51

Table 2: The mean and $1\text{-}\sigma$ constraints obtained for the models considered in section 3 using combined Planck 2018 + BAO + Pantheon observational data, in the non-phantom regime for the C/DDE parametrizations.

Fig. 2 highlights the major cosmological parameters of our concern. We note the following:

- In comparison to Λ CDM, all the DE parametrizations exhibit a reduced level of correlation between H_0 and Ω_{m0} .
- The strong correlation between $\sigma_{8,0}$ and H_0 is somewhat alleviated, with $\sigma_{8,0}$ preferring higher values than in Λ CDM. However, there is no shift in the values of H_0 , with the best-fit values remaining consistent with early-time estimations for Λ CDM.
- Ω_{m0} and $\sigma_{8,0}$ correlation is preserved. All C/DDE cases favour a lower Ω_{m0} value, and hence a higher value of $\sigma_{8,0}$.

Fig. 3 illustrates the effect of the interaction parameter. It reveals the following:

- The correlation between H_0 and Q is negligible for all models except Λ CDM.
- There is a strong positive correlation between Ω_{m0} and Q . All models in the non-phantom regime prefer an energy flow from the DM to the DE sector.

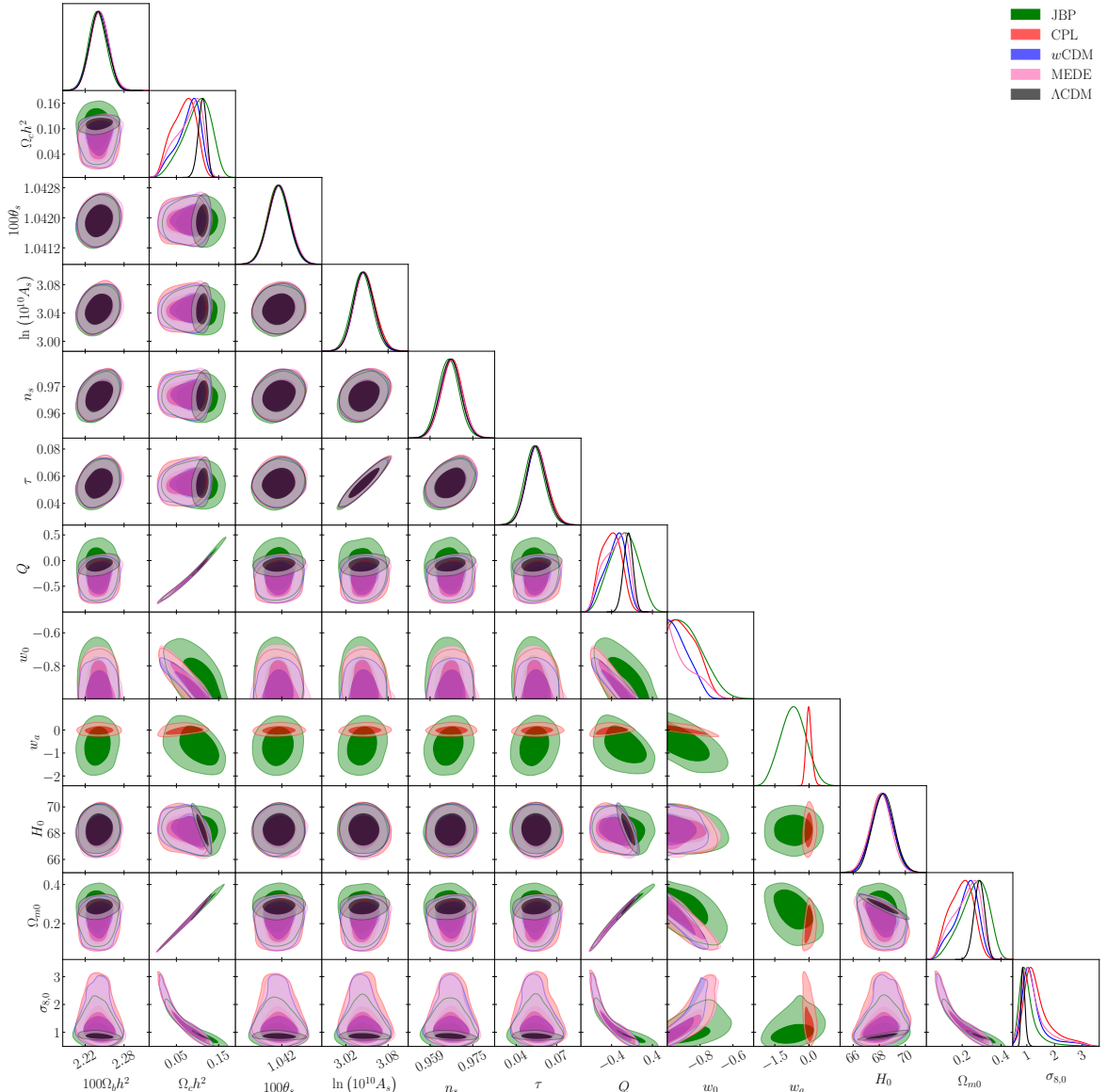


Figure 1: Comparison of constraints obtained for the models considered in section 3 using combined Planck 2018 + BAO + Pantheon observational data, in the non-phantom regime for the C/DDE parametrizations ($c_s^2 = 1$).

- The parameters, $\sigma_{8,0}$ and Q exhibit a strong negative correlation, leading to a preference for negative Q values, which in turn increases $\sigma_{8,0}$.

Finally, Fig. 4 depicts the effect of the EoS parameters. We find:

- There is almost no correlation between w_0 and H_0 , with H_0 centred around the early-time measurement.
- w_0 shows a strong negative correlation with Q , and hence a negative interaction prefers a more non-phantom nature.
- w_0 and w_a are seen to be slightly negatively correlated.

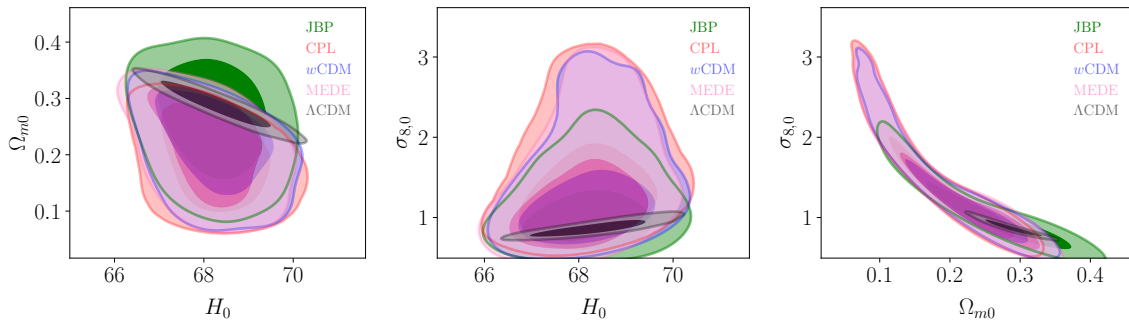


Figure 2: Constraints on and correlations between H_0 , Ω_{m0} and $\sigma_{8,0}$ in the non-phantom regime.

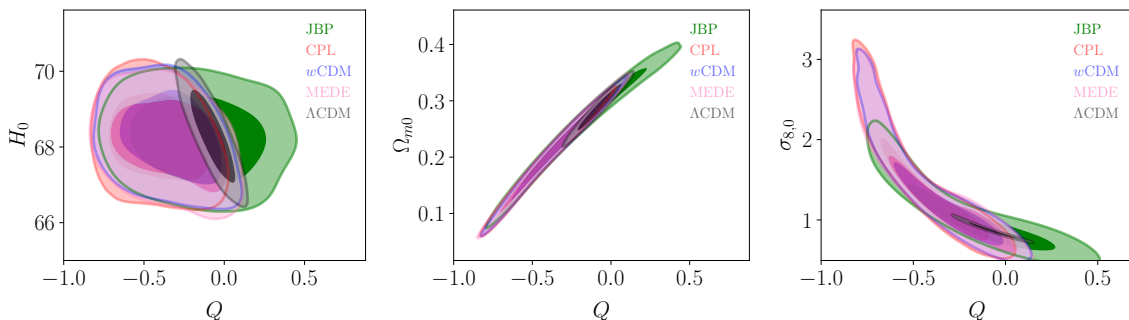


Figure 3: Constraints on and correlations of Q vs H_0 , Ω_{m0} and $\sigma_{8,0}$ in the non-phantom regime.

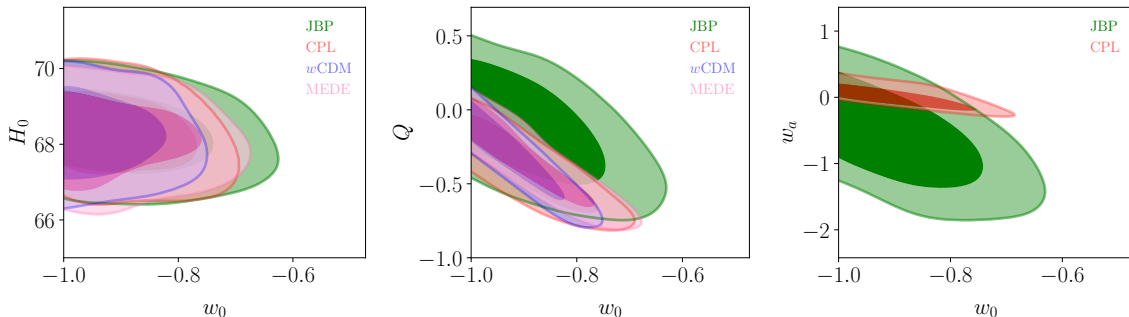


Figure 4: Constraints on and correlations of w_0 vs H_0 , Q and w_a in the non-phantom regime.

Based on these findings, we can infer that an interaction that allows energy transfer from the DM sector to the DE sector is favoured if the EoS is non-phantom. However, the most crucial point to note here is the value of $\sigma_{8,0}$ in Table 2. Generically, for any beyond- Λ CDM model, $\sigma_{8,0}$ takes a very large value, leading to overproduction of structures, which is naturally unrealistic and hence is not acceptable. Consequently, this tends to worsen the tension in $\sigma_{8,0}$ for all the C/DDE models, although the constraints on H_0 remain unaffected, indicating no improvement over the Hubble tension. This is mostly because of the very unrealistic value for the interaction term. So, although the presence of this interaction term helps in breaking the correlation between the parameters H_0 and $\sigma_{8,0}$, the non-phantom EoS fails miserably to address the $\sigma_{8,0}$ tension in the interacting scenario, generically for all the DE models here.

4.2 Phantom regime for DE

Table 3 presents the constraints on the interacting models considered in the phantom regime. For detailed visualisations, refer to the full triangle plots in Fig. 5.

Parameters	Λ CDM	w CDM	MEDE	CPL	JBP
$\Omega_b h^2$	0.02241 ± 0.00014	0.02241 ± 0.00014	0.02240 ± 0.00014	0.02239 ± 0.00014	0.02241 ± 0.00014
$\Omega_c h^2$	$0.111_{-0.0089}^{+0.010}$	0.133 ± 0.014	$0.129_{-0.021}^{+0.013}$	$0.143_{-0.011}^{+0.016}$	$0.135_{-0.014}^{+0.023}$
$100\theta_s$	1.04192 ± 0.00029	1.04193 ± 0.00028	1.04191 ± 0.00030	1.04190 ± 0.00028	1.04192 ± 0.00028
$\ln(10^{10} A_s)$	3.046 ± 0.015	3.045 ± 0.014	3.045 ± 0.014	3.043 ± 0.014	3.046 ± 0.015
n_s	0.9666 ± 0.0039	0.9662 ± 0.0039	0.9661 ± 0.0039	0.9656 ± 0.0038	0.9663 ± 0.0041
τ	0.0549 ± 0.0075	0.0544 ± 0.0073	0.0545 ± 0.0072	0.0537 ± 0.0074	0.0550 ± 0.0076
Q	-0.075 ± 0.092	0.14 ± 0.15	$0.10_{-0.22}^{+0.12}$	$0.24_{-0.13}^{+0.17}$	$0.17_{-0.17}^{+0.22}$
w_0	-	$-1.077_{-0.032}^{+0.068}$	$-1.065_{-0.029}^{+0.056}$	$-1.074_{-0.024}^{+0.072}$	$-1.11_{-0.032}^{+0.11}$
w_a	-	-	-	$-0.16_{-0.14}^{+0.21}$	$0.15_{-0.57}^{+0.50}$
H_0	68.32 ± 0.80	68.44 ± 0.80	68.64 ± 0.89	68.57 ± 0.81	68.50 ± 0.82
Ω_{m0}	0.288 ± 0.027	$0.334_{-0.032}^{+0.037}$	$0.324_{-0.048}^{+0.033}$	$0.353_{-0.026}^{+0.037}$	$0.337_{-0.032}^{+0.051}$
$\sigma_{8,0}$	$0.869_{-0.082}^{+0.054}$	$0.763_{-0.084}^{+0.050}$	0.785 ± 0.080	$0.726_{-0.069}^{+0.036}$	$0.760_{-0.11}^{+0.040}$
S_8	$0.845_{-0.028}^{+0.033}$	$0.797_{-0.030}^{+0.037}$	$0.809_{-0.040}^{+0.038}$	$0.780_{-0.024}^{+0.031}$	$0.789_{-0.030}^{+0.047}$
χ^2_{min}	3811	3810	3810	3810	3810
$-\ln \mathcal{L}_{min}$	1905.64	1905.12	1904.88	1904.97	1904.97

Table 3: The mean and 1- σ constraints obtained for the models considered in section 3 using combined Planck 2018 + BAO + Pantheon observational data, in the phantom regime for the different DE parametrizations.

As in the previous subsection, we separately highlight some of the parameters in Fig. 6, 7 and 8, in order to help us in the analysis. In Fig. 6 we observe the following trends:

- All the DE parametrizations exhibit reduced correlation between H_0 and Ω_{m0} compared to Λ CDM.
- The strong positive correlation between H_0 and $\sigma_{8,0}$ is relaxed in all the models in comparison to Λ CDM. This accommodates lower values of $\sigma_{8,0}$ without any considerable increase in H_0 .
- The correlation between Ω_{m0} and $\sigma_{8,0}$ is preserved, with all C/DDE cases favouring higher values of Ω_{m0} and consequently lower values of $\sigma_{8,0}$.

Fig. 7 illustrates the following:

- The correlation between H_0 and Q is eliminated for all the interacting models except Λ CDM.
- There is a strong positive correlation between Ω_{m0} and Q . Unlike Λ CDM, all C/DDE models in the phantom regime indicate an energy flow from DE to DM.
- $\sigma_{8,0}$ and Q exhibit a strong negative correlation. Therefore, a preference for a positive Q contributes to a reduction in $\sigma_{8,0}$.

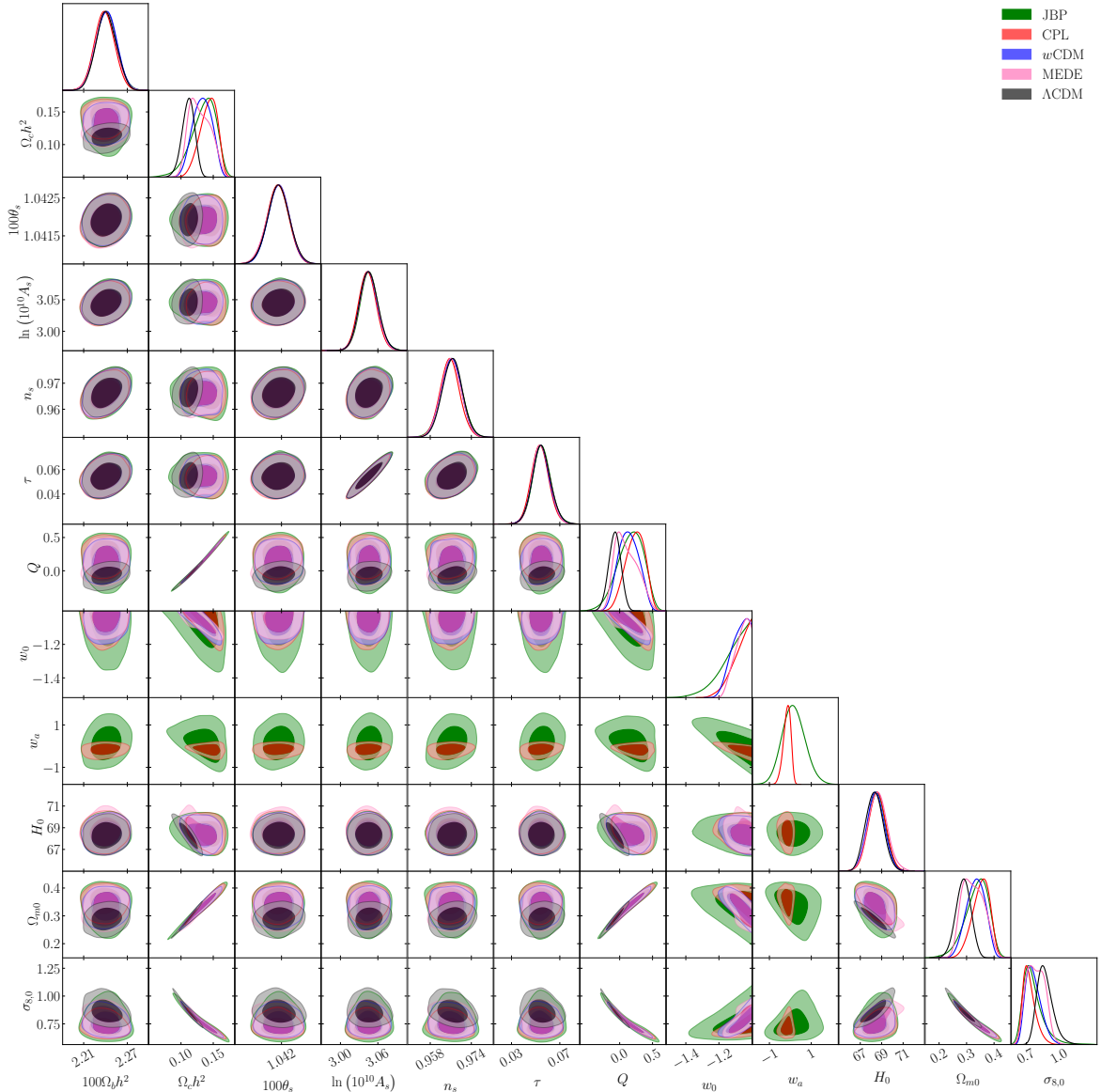


Figure 5: Comparison of constraints obtained for the models considered in section 3 using combined Planck 2018 + BAO + Pantheon observational data, in the phantom regime for the C/DDE parametrizations ($c_s^2 = 1$).

In Fig. 8 we find:

- There exists almost zero correlation between w_0 and H_0 , with H_0 centred around the early-time measurement.
- w_0 exhibits a negative correlation with Q , indicating that a positive interaction favours a more phantom-like behaviour. However, w_a does not show any significant correlation with Q .
- The DE EoS parameters, w_0 and w_a , are negatively correlated.

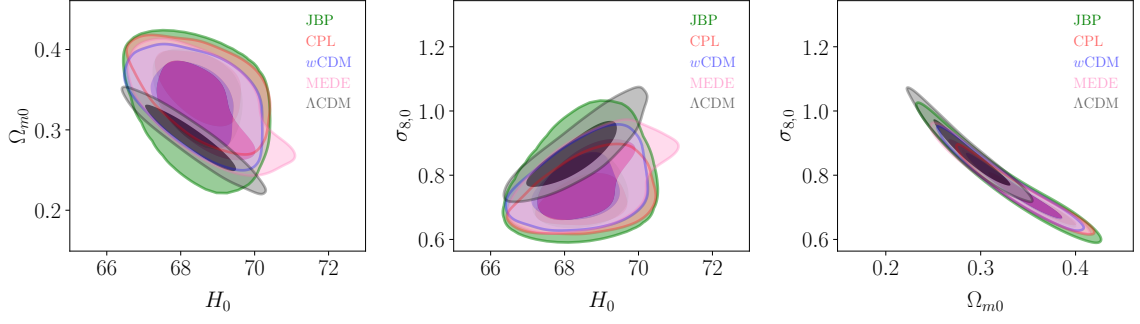


Figure 6: Constraints on and correlations between H_0 , Ω_{m0} and $\sigma_{8,0}$ in the phantom regime.

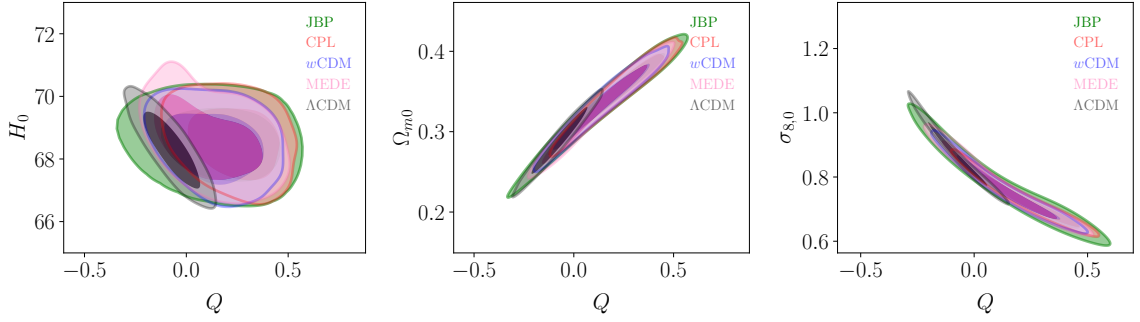


Figure 7: Constraints on and correlations of Q vs H_0 , Ω_{m0} and $\sigma_{8,0}$ in the phantom regime.

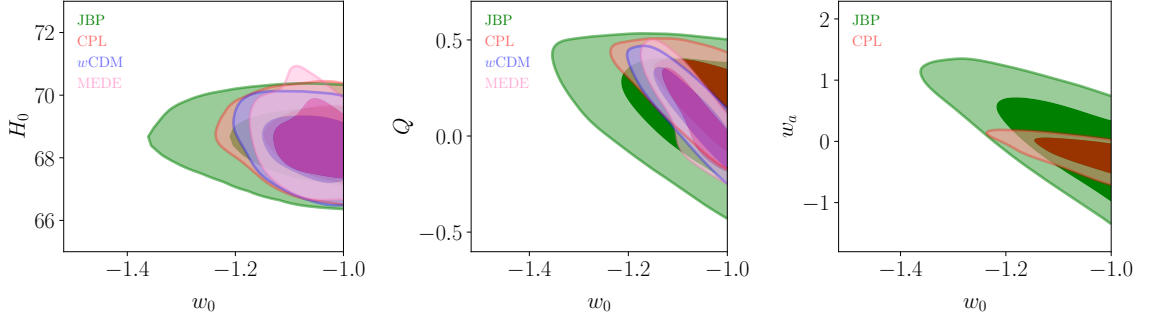


Figure 8: Constraints on and correlations of w_0 vs H_0 , Q and w_a in the phantom regime.

Based on these observations, we find that an interaction that promotes energy transfer from the DE sector to the DM sector is favoured in the phantom scenario. This in turn helps lower the constraints on $\sigma_{8,0}$, thereby leading to chances of alleviating the clustering tension. Nevertheless, it does not lead to any unrealistic value for any of the parameters under consideration. It is important to note that the constraints on H_0 although still in tension with the late-time measurements, show the possibility of slight improvement (unlike the substantial improvement in $\sigma_{8,0}$) with simultaneous lowering of clustering tension.

4.3 Comparison and interpretation

Let us now engage ourselves in a comparison of the outcome of phantom versus non-phantom regimes for the models under consideration. Our analysis reveals that an interacting scenario with a phantom DE sector helps in relaxing the clustering tension, with a slight improvement of the Hubble tension. This effect is achieved through a joint relaxation of the correlations between $H_0 - \Omega_{m0}$ and $H_0 - \sigma_{8,0}$, enabling Ω_{m0} and $\sigma_{8,0}$ to vary without inducing significant shifts in H_0 . Interestingly, H_0 appears to lose its correlation to the interaction parameter Q in the presence of the diverse EoS parametrization of DE. Strong correlations notably influence the behaviour of $\sigma_{8,0}$, while all DE models exhibit a negative correlation between w_0 and Q , indicating that a more phantom nature prefers higher values of Q . Given the existing degeneracy between Ω_{m0} and $\sigma_{8,0}$, this causes an increase in Ω_{m0} and a decrease in σ_8 due to their positive and negative correlations with Q , respectively. Such trends are also reflected in the positive correlation between Ω_{m0} and $\sigma_{8,0}$.

All correlations between the parameters are identically maintained for the non-phantom cases. However, the key difference arises due to the non-phantom nature of EoS, wherein w_0 is correlated with increasingly negative values of Q as the model diverges further from a cosmological constant. This, in turn, leads to a decrease in $\Omega_{m,0}$ and an increase in $\sigma_{8,0}$, exacerbating the clustering tension. Nonetheless, H_0 remains quite largely unaffected for the non-phantom scenario.

A closer examination of the observed correlations reveals that a positive Q implies an injection of energy into the matter sector, thereby increasing the value of Ω_{m0} . As Ω_{m0} and $\sigma_{8,0}$ are strongly degenerate, an increase in the value of Ω_{m0} is complemented with a decrease in $\sigma_{8,0}$. This is reflected through a negative correlation between $\sigma_{8,0}$ and Q . The inclusion of the Pantheon SNIa data puts tight constraints on the parameter space $w_0 - w_a$ of the CPL and JBP models, with the presence of a strong negative correlation between w_0 and w_a for both the phantom and non-phantom regimes. In all non- Λ CDM interacting DE models, there exists a negative correlation between Ω_{m0} and w_0 , with an almost negligible correlation between Ω_{m0} and w_a , similar to non-interacting models. This observation strongly supports the negative correlation between Q and w_0 . Consequently, H_0 becomes decoupled from other cosmological parameters, such as Ω_{m0} and w_0 , remaining mostly unaffected by shifts in these parameters in the presence of interacting scenarios for both the phantom and non-phantom regimes.

It is important to note that in all the cases considered, a non-interacting scenario ($Q = 0$) is always included at a 2σ confidence level, irrespective of the phantom or non-phantom nature of DE. Nonetheless, the presence of a mild non-zero interaction cannot be ruled out for some models within the 1σ confidence level. These DE parametrizations, in phantom *vs* non-phantom limit, propose different scenarios for the interaction between the dark sectors, leading to different predictions for the direction of energy flow. In our work, a positive Q indicates a transfer of energy from the DE to the DM sector implying that DE decays or converts into DM over cosmic time, whereas a negative Q indicates the reverse, *i.e.* an energy flow from the DM to the DE sector. We find that a phantom DE EoS favours an energy flow from the DE to the DM sector, whereas a non-phantom EoS for DE predicts a transfer of energy from the DM to the DE sector.

For the datasets under consideration, we observe a slight preference for phantom models over their non-phantom counterparts, as indicated by the χ^2 and $-\ln \mathcal{L}_{\min}$ values. Although this improvement in χ^2 values for phantom models is minor and should not be taken too seriously, it suggests a slightly better fit to observational data than non-phantom DE cases.

Parameters	Λ CDM	w CDM	MEDE	CPL	JBP
S_8	$0.845^{+0.033}_{-0.028}$ (2.33 σ)	$0.797^{+0.037}_{-0.030}$ (0.98 σ)	$0.809^{+0.038}_{-0.040}$ (1.08 σ)	$0.780^{+0.031}_{-0.024}$ (0.62 σ)	$0.789^{+0.047}_{-0.030}$ (0.78 σ)
H_0	$68.314^{+0.796}_{-0.821}$ (3.57 σ)	$68.436^{+0.807}_{-0.772}$ (3.55 σ)	$68.626^{+0.868}_{-0.873}$ (3.25 σ)	$68.571^{+0.815}_{-0.818}$ (3.38 σ)	$68.509^{+0.802}_{-0.812}$ (3.43 σ)

Table 4: Indicative Gaussian tension metric values for the various models under study in the phantom regime. The tensions are computed against the late-time H_0 measurement by SH0ES [80] ($H_0 = 73.04 \pm 1.04$) and the late-time $S_8/\sigma_{8,0}$ measurement from DES-Y3 [19] ($S_8 = 0.759^{+0.025}_{-0.023}/\sigma_{8,0} = 0.783^{+0.073}_{-0.092}$), which are themselves in tension with early-time measurements assuming vanilla Λ CDM ($H_0 = 67.744^{+0.406}_{-0.419}$, $\sigma_{8,0} = 0.810^{+0.006}_{-0.006}$, $S_8 = 0.824^{+0.010}_{-0.010}$), at $\sim 5\sigma$ and $\sim 3\sigma$ respectively.

While the non-phantom scenario indicates unrealistically high values for $\sigma_{8,0}$ which will eventually jeopardise structure formation by overproduction, phantom DE models lower the value of $\sigma_{8,0}$ that helps relax the S_8 tension without disturbing the other parameters significantly. Furthermore, phantom DE models not only demonstrate an improvement in the S_8 parameter but also show a slight shift towards higher H_0 values, which can help reconcile the Hubble tension thus addressing multiple cosmological tensions simultaneously. This capacity to offer a more coherent explanation for various observational datasets strengthens the case for phantom DE. These results align with previous findings (see [22]) that a phantom EoS for DE, with energy flow from DE to DM, is slightly favoured based on current data. Overall, our analysis suggests that phantom DE models provide a more accurate description of the observed Universe and are marginally preferred over non-phantom models for the current combination of datasets.

Table 4 summarises the extent of tension for both S_8 and H_0 for all the models under consideration. It can be found that an interacting scenario with the cosmological constant is not helpful with the S_8 tension. However, C/DDE interacting scenarios greatly help in relaxing the S_8 tension to $\lesssim 1\sigma$, with CPL performing the best followed closely by JBP, and then w CDM and MEDE. Moreover, we note that a parametrization with two free parameters performs better than one free parameter only. For the Hubble tension, we see all the interacting scenarios to perform equally well, and alleviate the same to $\sim 3.5\sigma$. Although this is not a fully satisfactory outcome, it is quite intriguing that these models (with the exception of interacting Λ CDM) tend to alleviate the S_8 tension this well, and also somewhat ease the H_0 tension, rather than exacerbating it. This is thanks to the reduction, and in some cases complete nullification, of the correlation of H_0 with $\sigma_{8,0}$ and $\Omega_{m,0}$.

4.4 Any effect of keeping c_s^2 free?

The sound speed of DE can influence the evolution of cosmological perturbations and, consequently, observables such as the CMB power spectrum or large-scale structure (LSS) observations. In order to examine any effect of that in the present analysis, we run the code afresh with the same models and same datasets, this time keeping the DE sound speed free. We find that c_s^2 remains largely unconstrained, *i.e.* it cannot be precisely probed by the given combination of datasets. The behaviour of DE for the above models is fairly consistent for the given range of c_s^2 values, indicating its degeneracy with other cosmological parameters. The lack of strong constraints on the sound speed also implies that the overall predictions

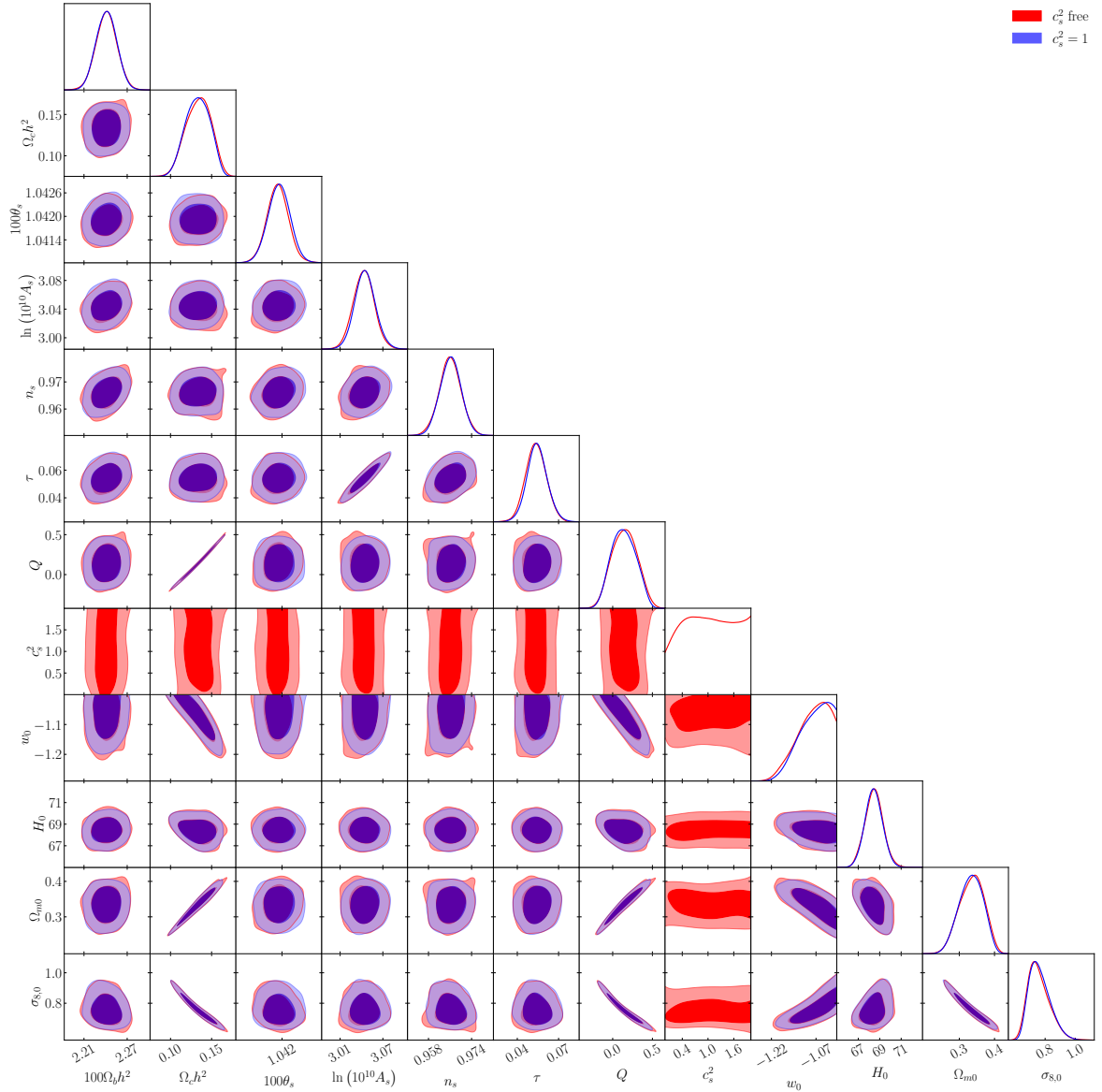


Figure 9: Comparison of constraints obtained for the w CDM model using combined Planck 2018 + BAO + Pantheon observational data, in the phantom regime, once by fixing $c_s^2 = 1$, and once by keeping it as a free parameter in the MCMC analysis.

of these iDMDE models are not overly sensitive to the specific value of c_s^2 in the considered range. Therefore, we find that for all the cases under study, keeping c_s^2 as a free parameter does not help in relaxing any tensions, doesn't affect any correlations significantly nor are there significant variations in the constraints of all the other parameters. As a demonstrative example, we show in Fig. 9 and Table 5 the comparison between the constraints for the w CDM phantom interacting case, for $c_s^2 = 1$ and c_s^2 open, highlighting these features.

Parameters	$c_s^2 = 1$	c_s^2 free
$\Omega_b h^2$	0.02241 ± 0.00014	0.02241 ± 0.00015
$\Omega_c h^2$	0.133 ± 0.014	$0.134^{+0.016}_{-0.015}$
$100\theta_s$	1.04193 ± 0.00028	1.04189 ± 0.00027
$\ln(10^{10} A_s)$	3.045 ± 0.014	3.043 ± 0.015
n_s	0.9662 ± 0.0039	0.9661 ± 0.0040
τ	0.0544 ± 0.0073	0.0536 ± 0.0075
Q	0.14 ± 0.15	0.15 ± 0.16
c_s^2	-	unconstrained
w_0	$-1.077^{+0.068}_{-0.032}$	$-1.082^{+0.065}_{-0.037}$
H_0	68.44 ± 0.80	68.47 ± 0.84
Ω_{m0}	$0.334^{+0.037}_{-0.032}$	$0.336^{+0.038}_{-0.033}$
$\sigma_{8,0}$	$0.763^{+0.050}_{-0.084}$	$0.758^{+0.052}_{-0.085}$
S_8	$0.797^{+0.037}_{-0.030}$	$0.793^{+0.038}_{-0.029}$

Table 5: The mean and 1- σ constraints obtained for the w CDM model using combined Planck 2018 + BAO + Pantheon observational data, in the phantom regime, once by fixing $c_s^2 = 1$, and once by keeping it as a free parameter in the MCMC analysis.

5 Possible role of $f\sigma_8$ RSD data

The clustering parameter $\sigma_{8,0}$ is related to $f\sigma_8$ which is probed by RSD data. Here f is the growth rate of structure formation, which in the interacting dark scenario is given as [90],

$$f \equiv \frac{d \ln \delta_m}{d \ln a} = \frac{\mathcal{H}^{-1}}{\delta_m} \left(\frac{\dot{\delta}_c \rho_c + \dot{\delta}_b \rho_b}{\rho_m} + \delta_c \frac{aQ}{\rho_m} - \delta_m \frac{aQ}{\rho_m} \right). \quad (5.1)$$

Here, the evolution of the matter density contrast δ_m , in a linearised approximation, is given by [91],

$$\delta_m'' + \left(\frac{3}{a} + \frac{H'}{H} \right) \delta_m' - \frac{3}{2} \frac{\Omega_{m0}}{a^5 H^2} \delta_m = 0, \quad (5.2)$$

where $H = a^{-1} \mathcal{H}$, such that

$$H^2 = H_0^2 \left[\Omega_{m0} a^{-3} + (1 - \Omega_{m0}) \left(a^{-3} Q \int_1^a \frac{a'^2 e^{\xi(a')}}{a'^Q} da' + \frac{e^{\xi(a)}}{a^Q} \right) \right], \quad (5.3)$$

and, $\xi(a) = \int_a^1 \frac{3[1+w(a')]}{a'} da'$.

Equation (5.1) is a consequence of the non-similar evolution of CDM and baryons in the presence of interactions. The standard scenario is restored for a null interaction term. Observationally f does not promise to be a very reliable quantity given its dependence on the bias parameter which relates tracers of matter (such as luminous galaxies) with the underlying total matter distribution ($\delta_g = b\delta_m$). In this regard, a more dependable quantity is the product $f(z)\sigma_8(z)$, where $\sigma_8(z)$ is the root mean square of mass fluctuations within a sphere of radius $R = 8h^{-1}$ Mpc defined as follows,

$$\sigma^2(R, z) = \frac{1}{2\pi^2} \int_0^\infty k^2 P(k, z) W(kR)^2 dk, \quad (5.4)$$

where $P(k, z)$ is the power spectrum, and $W(kR)$ is a top-hat window function. We proceed to investigate the effects the $f\sigma_8$ datasets from RSD would have on the clustering parameter.

Parameters	Λ CDM	w CDM	MEDE	CPL	JBP
$\Omega_b h^2$	0.02247 ± 0.00014	0.02241 ± 0.00014	$0.02241^{+0.00015}_{-0.00014}$	0.02239 ± 0.00014	0.02242 ± 0.00014
$\Omega_c h^2$	0.1236 ± 0.0020	$0.1251^{+0.0019}_{-0.0022}$	$0.1254^{+0.0017}_{-0.0025}$	0.1255 ± 0.0021	0.1248 ± 0.0026
$100\theta_s$	$1.04196^{+0.00031}_{-0.00027}$	1.04191 ± 0.00030	$1.04189^{+0.00032}_{-0.00026}$	1.04190 ± 0.00029	1.04194 ± 0.00029
$\ln(10^{10} A_s)$	3.049 ± 0.015	3.044 ± 0.015	3.045 ± 0.015	3.042 ± 0.014	3.046 ± 0.015
n_s	0.9682 ± 0.0037	0.9662 ± 0.0037	0.9663 ± 0.0040	0.9655 ± 0.0038	0.9667 ± 0.0038
τ	0.0574 ± 0.0074	0.0540 ± 0.0073	$0.0546^{+0.0083}_{-0.0073}$	0.0532 ± 0.0072	0.0554 ± 0.0076
Q	$0.044^{+0.017}_{-0.015}$	0.051 ± 0.016	$0.053^{+0.014}_{-0.017}$	$0.053^{+0.014}_{-0.016}$	0.051 ± 0.023
w_0	-	$-1.044^{+0.033}_{-0.017}$	$-1.046^{+0.034}_{-0.016}$	$-1.033^{+0.033}_{-0.0090}$	$-1.086^{+0.085}_{-0.024}$
w_a	-	-	-	$-0.094^{+0.12}_{-0.071}$	$0.28^{+0.28}_{-0.50}$
H_0	67.41 ± 0.55	$68.30^{+0.64}_{-0.76}$	$68.49^{+0.53}_{-0.90}$	68.61 ± 0.69	68.35 ± 0.79
Ω_{m0}	0.3230 ± 0.0086	0.3177 ± 0.0088	0.3174 ± 0.0083	0.3157 ± 0.0085	0.3166 ± 0.0098
$\sigma_{8,0}$	$0.7837^{+0.0088}_{-0.010}$	$0.7918^{+0.0097}_{-0.012}$	$0.7939^{+0.0088}_{-0.013}$	0.795 ± 0.011	0.791 ± 0.012
S_8	$0.812^{+0.011}_{-0.010}$	$0.814^{+0.010}_{-0.010}$	$0.814^{+0.011}_{-0.010}$	$0.815^{+0.010}_{-0.010}$	$0.812^{+0.010}_{-0.010}$
χ^2_{min}	3825	3824	3825	3824	3825
$-\ln \mathcal{L}_{min}$	1912.46	1912.15	1912.37	1912.09	1912.42

Table 6: The mean and $1\text{-}\sigma$ constraints obtained for all the models in the phantom regime, for $c_s^2 = 1$, using combined Planck 2018 + BAO + Pantheon observational data in addition to $f\sigma_8$ RSD data (compilation taken from [54]).

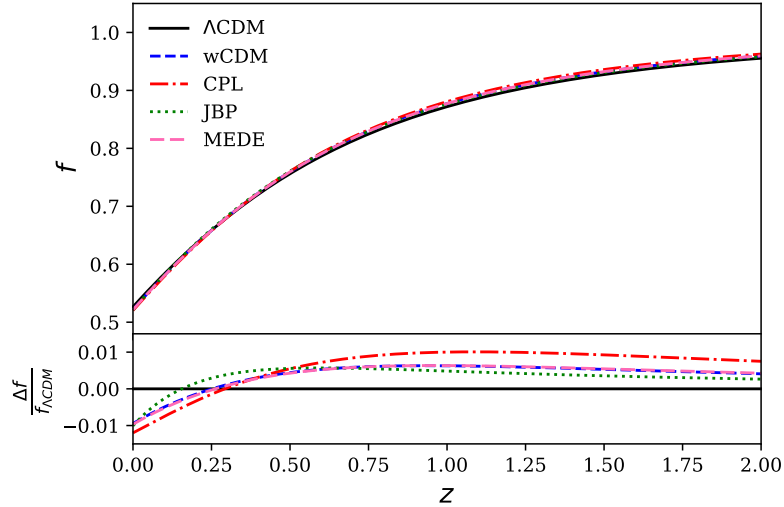


Figure 10: Plot of the redshift evolution of the growth factor for the different iDMDE with C/DDE scenarios considered in this work ($c_s^2 = 1$). Here $\Delta f = f_{\text{model}} - f_{\Lambda\text{CDM}}$ for the different iDMDE models under consideration

We consider the data compiled in [54]. We present the results for the different C/DDE cases in Table 6. Since we are dealing with C/DDE models, it is imperative to consider the possible non-trivial effects of these models in the growth equation to avoid biases toward Λ CDM. We carefully address this aspect in our analysis to strive for an unbiased assessment. For a

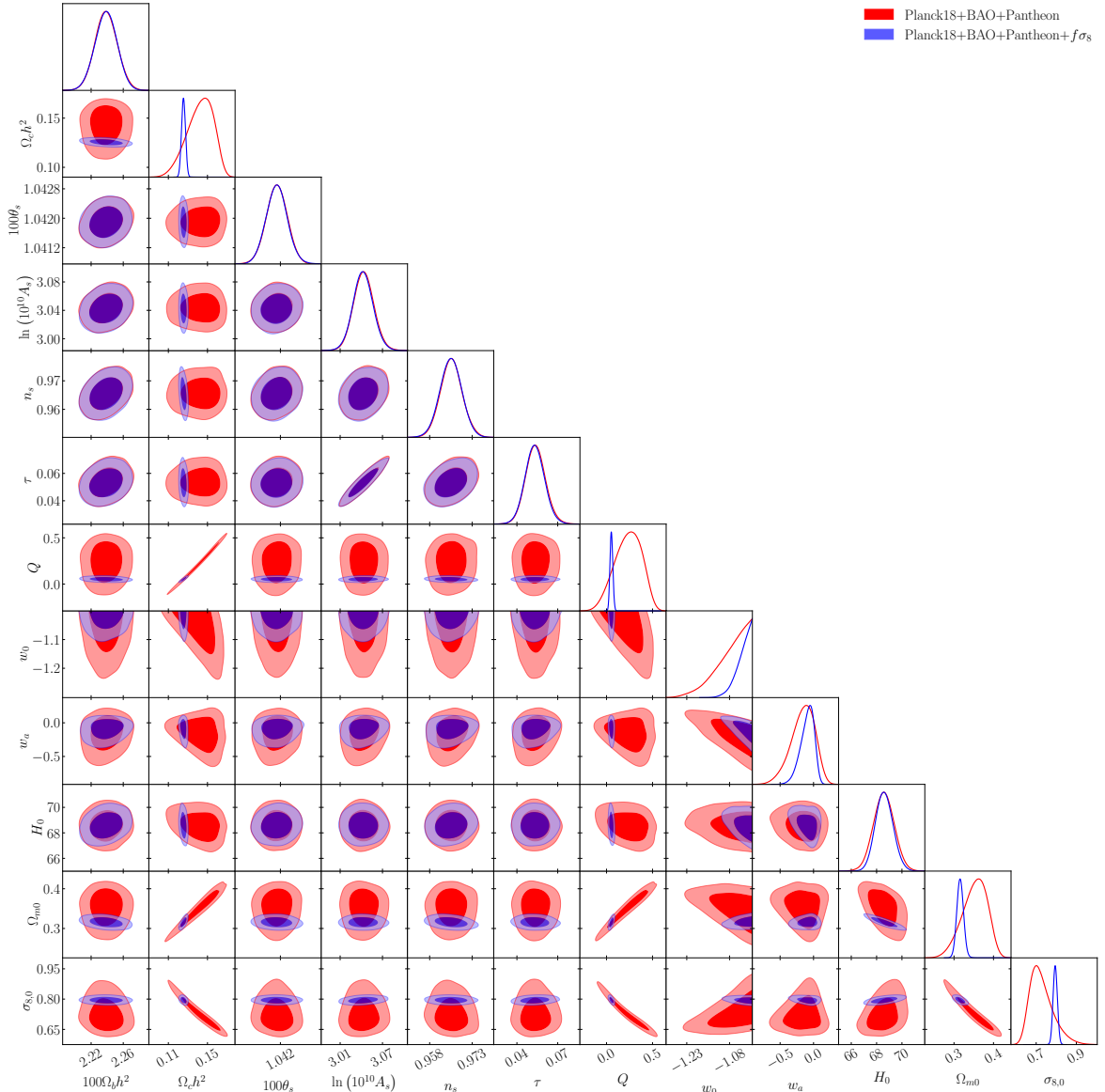


Figure 11: Comparison of constraints obtained for the CPL DE model in the phantom regime, for $c_s^2 = 1$, using combined Planck 2018 + BAO + Pantheon observational data, *vs* the addition of $f\sigma_8$ RSD data (compilation taken from [54]).

phantom DE EoS ($w_0 < -1$), Eq. (5.2) suggests an increase of the damping term at late times. This results in a lower value of δ_m , which in turn results in a lower rate of structure formation ($f = d \ln \delta_m / d \ln a$). In Fig. 10, we note that all the interacting C/DDE models prefer a lower value of the growth rate f today in the phantom regime, compared to the interacting Λ CDM model, which is consistent with the theoretical expectations. Since RSD observations constrain the product $f\sigma_8$, a corresponding increase in $\sigma_{8,0}$ is observed for the respective cases along with a decrease in value of Ω_{m0} compared to the ones presented in Table 3 while excluding the RSD data.

The comparison between results obtained with and without RSD data for the interacting CPL model is illustrated in Fig. 11. We see that the addition of the RSD data greatly improves

the constraints on certain parameters, with an order of magnitude increase in precision for Ω_{m0} and $\sigma_{8,0}$. The interaction parameter Q is also constrained better, with the possibility regarding the presence a non-zero Q at the 1σ confidence level. However, there is no appreciable shift in H_0 , similar to the previous phantom DE EoS scenarios. The joint constraints with the RSD data prefer higher values of S_8 , closer to those obtained from KiDS-450+GAMA ($S_8 = 0.800^{+0.029}_{-0.027}$ [20]) and HSC SSP ($S_8 = 0.804^{+0.032}_{-0.029}$ [21]). These constraints fall in between the late-time measurements by CFHTLenS ($S_8 = 0.732^{+0.029}_{-0.031}$ [10]), KiDS-450 ($S_8 = 0.745 \pm 0.039$ [11]) and DES-Y3 ($S_8 = 0.759^{+0.025}_{-0.023}$ [19, 92]) on one side *vs* the early Universe CMB Planck 2018 constraints ($S_8 = 0.832 \pm 0.013$ [9]) on the other side, with better precision.

6 DE interacting with warm DM

In all our analyses, we consistently treated DM as completely non-relativistic, characterised by a vanishing EoS. However, given the significance of the $\sigma_{8,0}$ parameter in our investigation, which quantifies perturbations in the matter sector, it is prudent to explore the impact of DM with a nontrivial EoS. We particularly focus on the warm dark matter models [93, 94]. These models have emerged as promising avenues for addressing small-scale phenomena associated with the large-scale structure of the Universe, including the core-cusp problem [95, 96], missing satellites problem [97, 98], and the too-big-to-fail problem [99, 100]. WDM models effectively dampen the power spectrum at smaller scales and represent a minimal extension to Λ CDM, offering a potential solution to these small-scale challenges [101, 102]. Such an extension involving the cosmological constant in an interacting scenario has been studied in [103]. Consequently, we proceed to investigate this setup within the DE setup to discern its impact on the $\sigma_{8,0}$ tension. For this, we introduce a free but constant EoS parameter for DM, w_{DM} , together with a $w = w_0$ parametrization for DE (we call this w WDM, in order to distinguish it from w CDM). This modifies the continuity equations as,

$$\dot{\rho}_{\text{dm}} + 3\mathcal{H}(1 + w_{\text{DM}})\rho_{\text{dm}} = a^2 Q_{\text{dm}}^0 = aQ, \quad (6.1)$$

$$\dot{\rho}_{\text{de}} + 3\mathcal{H}(1 + w_0)\rho_{\text{de}} = a^2 Q_{\text{de}}^0 = -aQ, \quad (6.2)$$

the solutions to which are modified as follows,

$$\rho_{\text{dm}} = \rho_{\text{dm},0} a^{-3(1+w_{\text{DM}})} + Q \frac{\rho_{\text{de},0} a^{-3}}{3w_0 + Q} (1 - a^{-3w_0 - Q}), \quad (6.3)$$

$$\rho_{\text{de}} = \rho_{\text{de},0} a^{-3(1+w_0+Q/3)}. \quad (6.4)$$

Parameters	w CDM	w WDM
$\Omega_b h^2$	0.02241 ± 0.00014	0.02235 ± 0.00014
$\Omega_c h^2$	0.133 ± 0.014	0.135 ± 0.015
$100\theta_s$	1.04193 ± 0.00028	1.04190 ± 0.00029
$\ln(10^{10} A_s)$	3.045 ± 0.014	3.046 ± 0.014
n_s	0.9662 ± 0.0039	0.9660 ± 0.0040
τ	0.0544 ± 0.0073	0.0543 ± 0.0074
Q	0.14 ± 0.15	0.16 ± 0.16
w_0	$-1.077^{+0.068}_{-0.032}$	$-1.068^{+0.066}_{-0.022}$
w_{DM}	-	$0.00036^{+0.00011}_{-0.00035}$
H_0	68.44 ± 0.80	68.57 ± 0.89
Ω_{m0}	$0.334^{+0.037}_{-0.032}$	$0.336^{+0.038}_{-0.033}$
$\sigma_{8,0}$	$0.763^{+0.050}_{-0.084}$	$0.758^{+0.048}_{-0.087}$
S_8	$0.797^{+0.037}_{-0.030}$	$0.793^{+0.037}_{-0.030}$

Table 7: The mean and $1\text{-}\sigma$ constraints obtained for the interacting $w = w_0$ DE model using combined Planck 2018 + BAO + Pantheon observational data, in the phantom regime, for $c_s^2 = 1$, drawing a comparison between the w CDM case and a w WDM case characterised by an extra EoS parameter w_{DM} .

Correspondingly, the perturbation equations in the synchronous gauge now read,

$$\begin{aligned} \dot{\delta}_{dm} = & - (1 + w_{DM}) \left(\theta_{dm} + \frac{\dot{h}}{2} \right) + \mathcal{H} Q \frac{\rho_{de}}{\rho_{dm}} (\delta_{de} - \delta_{dm}) + Q \frac{\rho_{de}}{\rho_{dm}} \left(\frac{kv_T}{3} + \frac{\dot{h}}{6} \right) \\ & + 3\mathcal{H}w_{DM} \left[\delta_{dm} + \left\{ 3(1 + w_{DM}) - Q \frac{\rho_{de}}{\rho_{dm}} \right\} \frac{\mathcal{H}\theta_{dm}}{k^2} \right], \end{aligned} \quad (6.5)$$

$$\dot{\theta}_{dm} = - \mathcal{H}\theta_{dm} \left(1 + \frac{Q}{1 + w_{DM}} \frac{\rho_{de}}{\rho_{dm}} \right), \quad (6.6)$$

$$\begin{aligned} \dot{\delta}_{de} = & - (1 + w_0) \left(\theta_{de} + \frac{\dot{h}}{2} \right) - Q \left(\frac{kv_T}{3} + \frac{\dot{h}}{6} \right) \\ & - 3\mathcal{H}(c_s^2 - w_0) \left[\delta_{de} + \left\{ 3(1 + w_0) + Q \right\} \frac{\mathcal{H}\theta_{de}}{k^2} \right], \end{aligned} \quad (6.7)$$

$$\dot{\theta}_{de} = - \mathcal{H} (1 - 3c_s^2) \theta_{de} + \frac{Q\mathcal{H}\theta_{de}}{1 + w_0} (1 + c_s^2) + \frac{k^2 c_s^2}{1 + w_0} \delta_{de}, \quad (6.8)$$

with the usual definitions of the terms. We present a comparison between the results of keeping w_{DM} free *vs* fixing it to $w_{DM} = 0$ (the non-relativistic CDM scenario) which is analogous to previous cases, in Fig. 12 and Table 7. The resulting posterior for w_{DM} shows a peak very close to $w_{DM} = 0$, with a very small upper bound for w_{DM} . This means that the existence of non-cold DM (albeit slight) in the Universe cannot be discarded. However, such a small number has practically no effect on the parameters of interest, and hence a WDM scenario coupled with an interacting DE setup seems unlikely to be more beneficial than the standard CDM cases when it comes to relaxing cosmological tensions. We expect similar outcomes for the other DE parametrizations considered in this study.

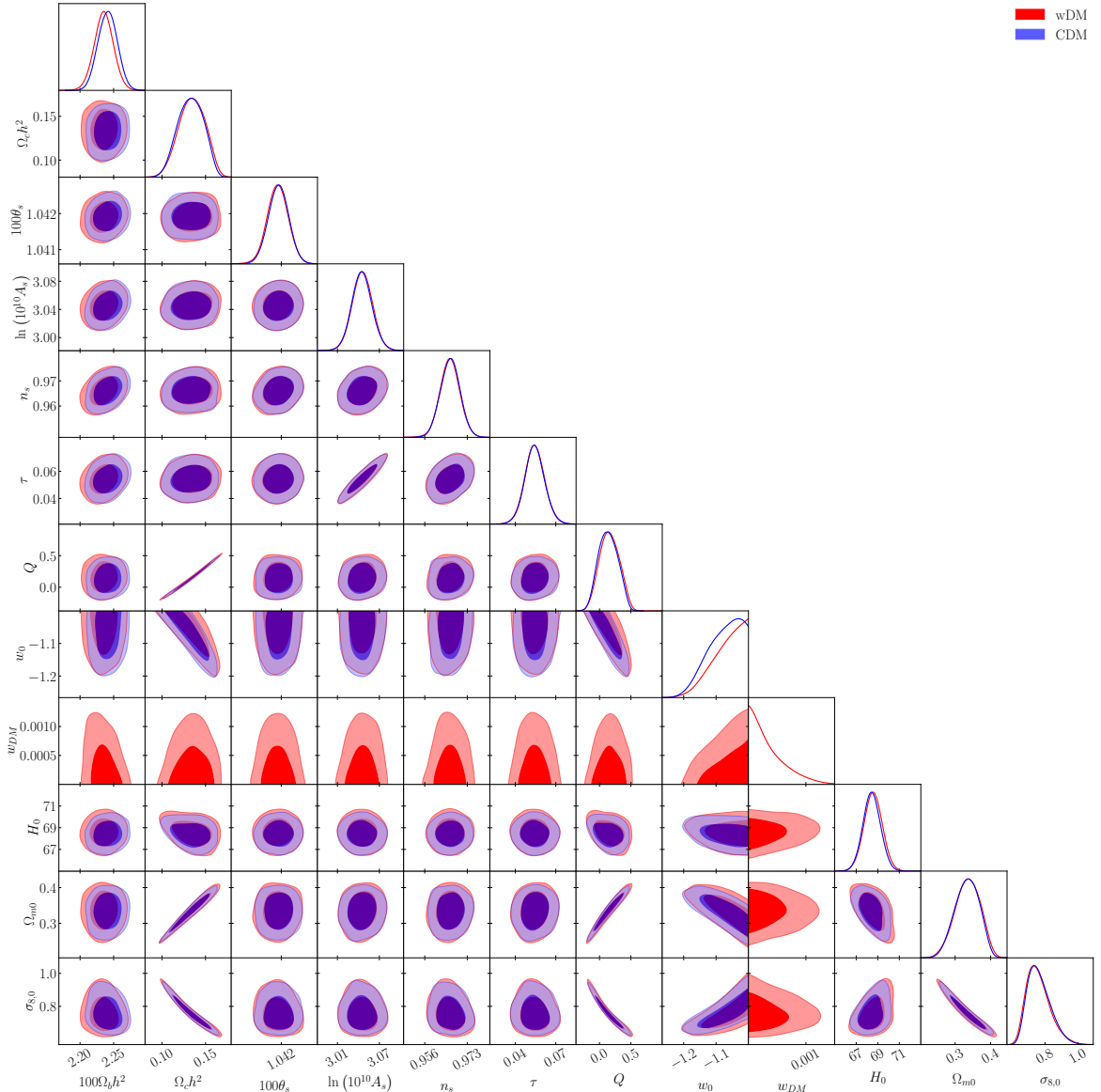


Figure 12: Comparison of constraints obtained for the interacting $w = w_0$ DE model using combined Planck 2018 + BAO + Pantheon observational data, in the phantom regime, for $c_s^2 = 1$, drawing a comparison between the w CDM case and a w WDM case characterised by an extra EoS parameter w_{DM} .

7 Conclusions

We re-investigate the viability of interacting dark matter and dark energy (iDMDE) models in addressing the clustering tension employing the latest CMB data from Planck 2018, BAO data, and the Pantheon SNIa compilation. Adopting an interaction term proportional to the dark energy density, we examine various parametrizations of the DE EoS for this interacting scenario. We incorporate the full impact of perturbations in both of the dark sectors, assuming that both dark matter and dark energy take part in clustering. The analysis has been undertaken for phantom and non-phantom regimes separately due to their distinct theoretical

motivations and to avoid phantom-crossing singularities in perturbation equations. We impose no additional constraints on other parameters, facilitating an agnostic data-driven analysis of the phantom and non-phantom sectors. Furthermore, examining both these scenarios independently can help in better understanding of how each different dark energy model impacts cosmological tensions and observational data, providing a more comprehensive analysis of these iDMDE models.

Our results indicate an elimination of the correlation between H_0 and $\sigma_{8,0}$ for interacting models with constant/dynamic DE EoS. In the phantom scenario, a positive interaction parameter Q (indicating energy flow from dark energy to dark matter) is preferred, with $\sigma_{8,0}$ showing a negative correlation with Q , thereby helping to reduce $\sigma_{8,0}$. Conversely, in the non-phantom regime, a negative interaction term is preferred. The same correlations observed in the phantom case also exist in the non-phantom scenario, nonetheless resulting in unrealistically large values of $\sigma_{8,0}$ resulting in an overproduction of structures, that lead to a worsening of the S_8 tension compared to Λ CDM, with apparently no shifts in the H_0 values. However, the phantom DE models can successfully alleviate the S_8 tension without exacerbating the H_0 tension. Besides improvement in S_8 values, the phantom models offer a slight shift towards higher H_0 values. This may, in principle, leave a provision of addressing multiple cosmological tensions simultaneously. Furthermore, a phantom EoS is favoured as a better fit to the current data sets. These findings point towards the superiority of the phantom models over the non-phantom ones, in the context of interactions in the dark sector and cosmological tensions.

To examine any effect of the sound speed of dark energy (c_s^2) in the present analysis, we reanalyse the iDMDE models keeping c_s^2 as a free parameter to be directly constrained from data. However, our findings indicate that the inclusion of c_s^2 as a free parameter has a negligible effect on overall constraints, suggesting that the current datasets are not sensitive to this parameter. This implies the robustness of our results subject to a wide range of possible c_s^2 values. We further investigated the role of the growth of structure ($f\sigma_8$) measurements from RSD data in addition to the aforementioned combination of datasets. We observe tighter constraints on certain parameters, resulting in a relatively less pronounced relaxation of the S_8 tension. This could imply the presence of an intrinsic bias towards Λ CDM in this dataset, where the data extraction is done by fixing the shape of the linear matter power spectrum by assuming a fiducial cosmology, highlighting the need for further investigation.

Additionally, we also investigate a scenario involving warm dark matter with a non-trivial equation of state (WDM) as an extension to the interacting cold dark matter - dark energy setup. Our results strongly favour the presence of cold dark matter (CDM) *viz.* $w_{\text{DM}} = 0$, with an upper bound obtained on w_{DM} in the interacting setup with a constant dark energy EoS. There are minimal shifts observed in constraints on the other parameters, including H_0 and S_8 . So this interacting warm dark matter dark energy setup has practically no effect on the parameters of interest. Thus, a WDM scenario coupled with an interacting DE setup seems unlikely to be more beneficial than the standard CDM cases when it comes to relaxing cosmological tensions.

It deserves mention that this whole exercise has been undertaken for the specific parametric form of the interaction term $\mathcal{Q} = HQ\rho_{\text{de}}$, where Q represents the coupling or strength of the interaction, as this particular form has previously shown promise in addressing the H_0 tension to some extent. However, open questions remain regarding the nature of the interaction term. The possibility of this Q evolving with redshift has been explored in [54], which calls for further investigation. As an alternative approach, one can attempt a non-parametric

reconstruction of \mathcal{Q} , where no prior dependence on the functional form exists. Some preliminary investigations have already begun in this direction [104–106]. However, a comprehensive analysis incorporating all combinations of data sets and their impact on the cosmological tensions is yet lacking, which we intend to investigate in future works.

Additionally, there are concerns regarding BAO data which rely on assuming a fiducial cosmology (typically the Λ CDM model) when extracting the BAO signal. This reliance on the fiducial template could introduce bias in the resulting parameter constraints for interacting models that significantly deviate from Λ CDM. Despite no specific model assumption with regard to the SNIa data, our analysis does assume that the intrinsic luminosities of SNIa do not evolve with redshift. This assumption of the constancy of the SNIa absolute magnitude M_B , a topic that has been widely debated (see [107]) can influence the constraints on other parameters during likelihood computation, potentially leading to significant differences in results. Investigating the applicability of these datasets to iDMDE models is crucial [29], especially given the uncertainty around the physical nature of the interaction parameter. These issues call for further exploration in future.

In conclusion, the introduction of interaction within the cosmic dark sector effectively eliminates the strong positive correlation existing between H_0 and $\sigma_{8,0}$ for non-interacting DM-DE models. A phantom EoS contributes to a reduction in the value of $\sigma_{8,0}$, thereby easing the clustering tension. Notably, the interacting CPL and JBP models, incorporating a phantom DE component, demonstrate the potential to alleviate the clustering tension to $< 1\sigma$ without exacerbating the Hubble tension, but rather relaxing it slightly. These results are intriguing as they suggest the potential to address both the S_8 and H_0 tensions simultaneously within the same theoretical framework. We hope to explore further in this direction in the future, considering more DE parametrizations with different combinations of datasets, and investigating the role that DE perturbations could play in light of future missions.

Data/Code availability: The datasets used in this work are all publicly available. The modified codes used for this study may be made available upon reasonable request.

Acknowledgments

We gratefully acknowledge the use of the publicly available codes *CLASS*, *MontePython* and *GetDist*. We thank Debarun Paul and Antara Dey for insightful discussions, and Arko Bhau-mik and Sourav Pal for invaluable support throughout the duration of this work. RS thanks ISI Kolkata for financial support through Senior Research Fellowship. PM acknowledges the financial support from ISI Kolkata and the Science & Engineering Research Board (SERB), Department of Science and Technology, Govt. of India under the National Post-Doctoral Fellowship (N-PDF File no. PDF/2023/001986). SP thanks the Department of Science and Technology, Govt. of India for partial support through Grant No. NMICPS/006/MD/2020-21. We acknowledge the computational facilities of ISI Kolkata, and those made available by the Technology Innovation Hub, ISI Kolkata.

References

- [1] D.K. Hazra, S. Majumdar, S. Pal, S. Panda and A.A. Sen, *Post-Planck Dark Energy Constraints*, *Phys. Rev. D* **91** (2015) 083005 [1310.6161].
- [2] B. Novosyadlyj, O. Sergijenko, R. Durrer and V. Pelykh, *Constraining the dynamical dark energy parameters: Planck-2013 vs WMAP9*, *JCAP* **05** (2014) 030 [1312.6579].

- [3] J.L. Bernal, L. Verde and A.G. Riess, *The trouble with H_0* , *JCAP* **10** (2016) 019 [[1607.05617](#)].
- [4] E. Di Valentino, O. Mena, S. Pan, L. Visinelli, W. Yang, A. Melchiorri et al., *In the realm of the Hubble tension—a review of solutions*, *Class. Quant. Grav.* **38** (2021) 153001 [[2103.01183](#)].
- [5] N. Schöneberg, G. Franco Abellán, A. Pérez Sánchez, S.J. Witte, V. Poulin and J. Lesgourgues, *The H_0 Olympics: A fair ranking of proposed models*, *Phys. Rept.* **984** (2022) 1 [[2107.10291](#)].
- [6] E. Abdalla et al., *Cosmology intertwined: A review of the particle physics, astrophysics, and cosmology associated with the cosmological tensions and anomalies*, *JHEAp* **34** (2022) 49 [[2203.06142](#)].
- [7] S. Vagnozzi, *Seven Hints That Early-Time New Physics Alone Is Not Sufficient to Solve the Hubble Tension*, *Universe* **9** (2023) 393 [[2308.16628](#)].
- [8] E. Di Valentino et al., *Cosmology Intertwined III: $f\sigma_8$ and S_8* , *Astropart. Phys.* **131** (2021) 102604 [[2008.11285](#)].
- [9] PLANCK collaboration, Planck 2018 results. VI. Cosmological parameters, *Astron. Astrophys.* **641** (2020) A6 [[1807.06209](#)].
- [10] S. Joudaki et al., *CFHTLenS revisited: assessing concordance with Planck including astrophysical systematics*, *Mon. Not. Roy. Astron. Soc.* **465** (2017) 2033 [[1601.05786](#)].
- [11] S. Joudaki et al., *KiDS-450: Testing extensions to the standard cosmological model*, *Mon. Not. Roy. Astron. Soc.* **471** (2017) 1259 [[1610.04606](#)].
- [12] S. Joudaki et al., *KiDS-450 + 2dFLenS: Cosmological parameter constraints from weak gravitational lensing tomography and overlapping redshift-space galaxy clustering*, *Mon. Not. Roy. Astron. Soc.* **474** (2018) 4894 [[1707.06627](#)].
- [13] H. Hildebrandt et al., *KiDS+VIKING-450: Cosmic shear tomography with optical and infrared data*, *Astron. Astrophys.* **633** (2020) A69 [[1812.06076](#)].
- [14] T. Tröster et al., *Cosmology from large-scale structure: Constraining Λ CDM with BOSS*, *Astron. Astrophys.* **633** (2020) L10 [[1909.11006](#)].
- [15] DES collaboration, *Dark Energy Survey Year 1 results: Cosmological constraints from cosmic shear*, *Phys. Rev. D* **98** (2018) 043528 [[1708.01538](#)].
- [16] S. Joudaki et al., *KiDS+VIKING-450 and DES-Y1 combined: Cosmology with cosmic shear*, *Astron. Astrophys.* **638** (2020) L1 [[1906.09262](#)].
- [17] KiDS collaboration, *KiDS-1000 Cosmology: Cosmic shear constraints and comparison between two point statistics*, *Astron. Astrophys.* **645** (2021) A104 [[2007.15633](#)].
- [18] C. Heymans et al., *KiDS-1000 Cosmology: Multi-probe weak gravitational lensing and spectroscopic galaxy clustering constraints*, *Astron. Astrophys.* **646** (2021) A140 [[2007.15632](#)].
- [19] DES collaboration, *Dark Energy Survey Year 3 results: Cosmology from cosmic shear and robustness to data calibration*, *Phys. Rev. D* **105** (2022) 023514 [[2105.13543](#)].
- [20] E. van Uitert et al., *KiDS+GAMA: cosmology constraints from a joint analysis of cosmic shear, galaxy–galaxy lensing, and angular clustering*, *Mon. Not. Roy. Astron. Soc.* **476** (2018) 4662 [[1706.05004](#)].
- [21] T. Hamana et al., *Cosmological constraints from cosmic shear two-point correlation functions with HSC survey first-year data*, *Publ. Astron. Soc. Jap.* **72** (2020) Publications of the Astronomical Society of Japan, Volume 72, Issue 1, February 2020, 16, <https://doi.org/10.1093/pasj/psz138> [[1906.06041](#)].

- [22] A. Bhattacharyya, U. Alam, K.L. Pandey, S. Das and S. Pal, *Are H_0 and σ_8 tensions generic to present cosmological data?*, *Astrophys. J.* **876** (2019) 143 [1805.04716].
- [23] L. Amendola, *Coupled quintessence*, *Phys. Rev. D* **62** (2000) 043511 [astro-ph/9908023].
- [24] W. Giarè, Y. Zhai, S. Pan, E. Di Valentino, R.C. Nunes and C. van de Bruck, *Tightening the reins on non-minimal dark sector physics: Interacting Dark Energy with dynamical and non-dynamical equation of state*, 2404.02110.
- [25] D. Benisty, S. Pan, D. Staicova, E. Di Valentino and R.C. Nunes, *Late-Time constraints on Interacting Dark Energy: Analysis independent of H_0 , r_d and M_B* , 2403.00056.
- [26] G.A. Hoerning, R.G. Landim, L.O. Ponte, R.P. Rolim, F.B. Abdalla and E. Abdalla, *Constraints on interacting dark energy revisited: implications for the Hubble tension*, 2308.05807.
- [27] M. Lucca and D.C. Hooper, *Shedding light on dark matter-dark energy interactions*, *Phys. Rev. D* **102** (2020) 123502 [2002.06127].
- [28] E. Di Valentino, A. Melchiorri and O. Mena, *Can interacting dark energy solve the H_0 tension?*, *Phys. Rev. D* **96** (2017) 043503 [1704.08342].
- [29] E. Di Valentino, A. Melchiorri, O. Mena and S. Vagnozzi, *Interacting dark energy in the early 2020s: A promising solution to the H_0 and cosmic shear tensions*, *Phys. Dark Univ.* **30** (2020) 100666 [1908.04281].
- [30] S. Pan and W. Yang, *On the interacting dark energy scenarios – the case for Hubble constant tension*, 2310.07260.
- [31] B. Wang, E. Abdalla, F. Atrio-Barandela and D. Pavón, *Further understanding the interaction between dark energy and dark matter: current status and future directions*, *Rept. Prog. Phys.* **87** (2024) 036901 [2402.00819].
- [32] W. Yang, S. Pan, E. Di Valentino, R.C. Nunes, S. Vagnozzi and D.F. Mota, *Tale of stable interacting dark energy, observational signatures, and the H_0 tension*, *JCAP* **09** (2018) 019 [1805.08252].
- [33] A. Bernui, E. Di Valentino, W. Giarè, S. Kumar and R.C. Nunes, *Exploring the H_0 tension and the evidence for dark sector interactions from 2D BAO measurements*, *Phys. Rev. D* **107** (2023) 103531 [2301.06097].
- [34] Y.-H. Yao and X.-H. Meng, *Can interacting dark energy with dynamical coupling resolve the Hubble tension*, *Phys. Dark Univ.* **39** (2023) 101165 [2207.05955].
- [35] S. Gariazzo, E. Di Valentino, O. Mena and R.C. Nunes, *Late-time interacting cosmologies and the Hubble constant tension*, *Phys. Rev. D* **106** (2022) 023530 [2111.03152].
- [36] R.-Y. Guo, L. Feng, T.-Y. Yao and X.-Y. Chen, *Exploration of interacting dynamical dark energy model with interaction term including the equation-of-state parameter: alleviation of the H_0 tension*, *JCAP* **12** (2021) 036 [2110.02536].
- [37] R.C. Nunes and E. Di Valentino, *Dark sector interaction and the supernova absolute magnitude tension*, *Phys. Rev. D* **104** (2021) 063529 [2107.09151].
- [38] L.-Y. Gao, Z.-W. Zhao, S.-S. Xue and X. Zhang, *Relieving the H_0 tension with a new interacting dark energy model*, *JCAP* **07** (2021) 005 [2101.10714].
- [39] S. Pan, W. Yang and A. Paliathanasis, *Non-linear interacting cosmological models after Planck 2018 legacy release and the H_0 tension*, *Mon. Not. Roy. Astron. Soc.* **493** (2020) 3114 [2002.03408].
- [40] H. Amirhashchi, A.K. Yadav, N. Ahmad and V. Yadav, *Interacting dark sectors in anisotropic universe: Observational constraints and H_0 tension*, *Phys. Dark Univ.* **36** (2022) 101043 [2001.03775].

- [41] S. Pan, W. Yang, E. Di Valentino, E.N. Saridakis and S. Chakraborty, *Interacting scenarios with dynamical dark energy: Observational constraints and alleviation of the H_0 tension*, *Phys. Rev. D* **100** (2019) 103520 [[1907.07540](#)].
- [42] S. Pan, W. Yang, C. Singha and E.N. Saridakis, *Observational constraints on sign-changeable interaction models and alleviation of the H_0 tension*, *Phys. Rev. D* **100** (2019) 083539 [[1903.10969](#)].
- [43] W. Yang, A. Mukherjee, E. Di Valentino and S. Pan, *Interacting dark energy with time varying equation of state and the H_0 tension*, *Phys. Rev. D* **98** (2018) 123527 [[1809.06883](#)].
- [44] L.-Y. Gao, S.-S. Xue and X. Zhang, *Dark energy and matter interacting scenario to relieve H_0 and S_8 tensions**, *Chin. Phys. C* **48** (2024) 051001 [[2212.13146](#)].
- [45] S. Kumar, R.C. Nunes and S.K. Yadav, *Dark sector interaction: a remedy of the tensions between CMB and LSS data*, *Eur. Phys. J. C* **79** (2019) 576 [[1903.04865](#)].
- [46] S. Kumar, *Remedy of some cosmological tensions via effective phantom-like behavior of interacting vacuum energy*, *Phys. Dark Univ.* **33** (2021) 100862 [[2102.12902](#)].
- [47] W. Yang, S. Pan, E. Di Valentino, O. Mena and A. Melchiorri, *2021- H_0 odyssey: closed, phantom and interacting dark energy cosmologies*, *JCAP* **10** (2021) 008 [[2101.03129](#)].
- [48] E. Di Valentino, A. Melchiorri, O. Mena and S. Vagnozzi, *Nonminimal dark sector physics and cosmological tensions*, *Phys. Rev. D* **101** (2020) 063502 [[1910.09853](#)].
- [49] M. Lucca, *Dark energy–dark matter interactions as a solution to the S_8 tension*, *Phys. Dark Univ.* **34** (2021) 100899 [[2105.09249](#)].
- [50] M. Chevallier and D. Polarski, *Accelerating universes with scaling dark matter*, *Int. J. Mod. Phys. D* **10** (2001) 213 [[gr-qc/0009008](#)].
- [51] R. An, C. Feng and B. Wang, *Relieving the Tension between Weak Lensing and Cosmic Microwave Background with Interacting Dark Matter and Dark Energy Models*, *JCAP* **02** (2018) 038 [[1711.06799](#)].
- [52] P. Mukherjee, A. Mukherjee, H.K. Jassal, A. Dasgupta and N. Banerjee, *Holographic dark energy: constraints on the interaction from diverse observational data sets*, *Eur. Phys. J. Plus* **134** (2019) 147 [[1710.02417](#)].
- [53] S. Sinha and N. Banerjee, *Density perturbation in an interacting holographic dark energy model*, *Eur. Phys. J. Plus* **135** (2020) 779 [[1911.06520](#)].
- [54] S. Sinha, *Differentiating dark interactions with perturbation*, *Phys. Rev. D* **103** (2021) 123547 [[2101.08959](#)].
- [55] S. Sinha, M. Banerjee and S. Das, *Perturbation in an interacting dark Universe*, *Phys. Dark Univ.* **42** (2023) 101273 [[2204.05174](#)].
- [56] PAN-STARRS1 collaboration, *The Complete Light-curve Sample of Spectroscopically Confirmed SNe Ia from Pan-STARRS1 and Cosmological Constraints from the Combined Pantheon Sample*, *Astrophys. J.* **859** (2018) 101 [[1710.00845](#)].
- [57] B. Wang, E. Abdalla, F. Atrio-Barandela and D. Pavon, *Dark Matter and Dark Energy Interactions: Theoretical Challenges, Cosmological Implications and Observational Signatures*, *Rept. Prog. Phys.* **79** (2016) 096901 [[1603.08299](#)].
- [58] W. Yang, S. Pan, R.C. Nunes and D.F. Mota, *Dark calling Dark: Interaction in the dark sector in presence of neutrino properties after Planck CMB final release*, *JCAP* **04** (2020) 008 [[1910.08821](#)].
- [59] N. Kaiser, *Clustering in real space and in redshift space*, *Mon. Not. Roy. Astron. Soc.* **227** (1987) 1.

- [60] S. Hannestad, *Constraints on the sound speed of dark energy*, *Phys. Rev. D* **71** (2005) 103519 [[astro-ph/0504017](#)].
- [61] J.-Q. Xia, Y.-F. Cai, T.-T. Qiu, G.-B. Zhao and X. Zhang, *Constraints on the Sound Speed of Dynamical Dark Energy*, *Int. J. Mod. Phys. D* **17** (2008) 1229 [[astro-ph/0703202](#)].
- [62] R. de Putter, D. Huterer and E.V. Linder, *Measuring the Speed of Dark: Detecting Dark Energy Perturbations*, *Phys. Rev. D* **81** (2010) 103513 [[1002.1311](#)].
- [63] M.S. Linton, A. Pourtsidou, R. Crittenden and R. Maartens, *Variable sound speed in interacting dark energy models*, *JCAP* **04** (2018) 043 [[1711.05196](#)].
- [64] B.R. Dinda and N. Banerjee, *Constraints on the speed of sound in the k-essence model of dark energy*, *Eur. Phys. J. C* **84** (2024) 177 [[2309.10538](#)].
- [65] G. Olivares, F. Atrio-Barandela and D. Pavon, *Observational constraints on interacting quintessence models*, *Phys. Rev. D* **71** (2005) 063523 [[astro-ph/0503242](#)].
- [66] J. Valiviita, E. Majerotto and R. Maartens, *Instability in interacting dark energy and dark matter fluids*, *JCAP* **07** (2008) 020 [[0804.0232](#)].
- [67] M.B. Gavela, L. Lopez Honorez, O. Mena and S. Rigolin, *Dark Coupling and Gauge Invariance*, *JCAP* **11** (2010) 044 [[1005.0295](#)].
- [68] A.A. Da Costa, *Observational Constraints on Models with an Interaction between Dark Energy and Dark Matter*, Ph.D. thesis, UFMA, Sao Luis, 2014.
- [69] C.-P. Ma and E. Bertschinger, *Cosmological perturbation theory in the synchronous and conformal Newtonian gauges*, *Astrophys. J.* **455** (1995) 7 [[astro-ph/9506072](#)].
- [70] E.V. Linder, *Exploring the expansion history of the universe [arXiv:0208512]*, *Phys. Rev. Lett.* **90** (2003) 091301 [[astro-ph/0208512](#)].
- [71] H.K. Jassal, J.S. Bagla and T. Padmanabhan, *Observational constraints on low redshift evolution of dark energy: How consistent are different observations?*, *Phys. Rev. D* **72** (2005) 103503 [[astro-ph/0506748](#)].
- [72] X. Li and A. Shafieloo, *A Simple Phenomenological Emergent Dark Energy Model can Resolve the Hubble Tension*, *Astrophys. J. Lett.* **883** (2019) L3 [[1906.08275](#)].
- [73] H.B. Benaoum, W. Yang, S. Pan and E. Di Valentino, *Modified emergent dark energy and its astronomical constraints*, *Int. J. Mod. Phys. D* **31** (2022) 2250015 [[2008.09098](#)].
- [74] PLANCK collaboration, *Planck 2018 results. V. CMB power spectra and likelihoods*, *Astron. Astrophys.* **641** (2020) A5 [[1907.12875](#)].
- [75] PLANCK collaboration, *Planck 2018 results. VIII. Gravitational lensing*, *Astron. Astrophys.* **641** (2020) A8 [[1807.06210](#)].
- [76] F. Beutler, C. Blake, M. Colless, D.H. Jones, L. Staveley-Smith, L. Campbell et al., *The 6dF Galaxy Survey: Baryon Acoustic Oscillations and the Local Hubble Constant*, *Mon. Not. Roy. Astron. Soc.* **416** (2011) 3017 [[1106.3366](#)].
- [77] A.J. Ross, L. Samushia, C. Howlett, W.J. Percival, A. Burden and M. Manera, *The clustering of the SDSS DR7 main Galaxy sample – I. A 4 per cent distance measure at $z = 0.15$* , *Mon. Not. Roy. Astron. Soc.* **449** (2015) 835 [[1409.3242](#)].
- [78] BOSS collaboration, *The clustering of galaxies in the completed SDSS-III Baryon Oscillation Spectroscopic Survey: cosmological analysis of the DR12 galaxy sample*, *Mon. Not. Roy. Astron. Soc.* **470** (2017) 2617 [[1607.03155](#)].
- [79] R. Shah, A. Bhaumik, P. Mukherjee and S. Pal, *A thorough investigation of the prospects of eLISA in addressing the Hubble tension: Fisher forecast, MCMC and Machine Learning*, *JCAP* **06** (2023) 038 [[2301.12708](#)].

- [80] A.G. Riess et al., *A Comprehensive Measurement of the Local Value of the Hubble Constant with $1 \text{ km s}^{-1} \text{ Mpc}^{-1}$ Uncertainty from the Hubble Space Telescope and the SH0ES Team*, *Astrophys. J. Lett.* **934** (2022) L7 [2112.04510].
- [81] J. Lesgourgues, *The Cosmic Linear Anisotropy Solving System (CLASS) I: Overview*, *arXiv:1104.2932* (2011) [1104.2932].
- [82] D. Blas, J. Lesgourgues and T. Tram, *The Cosmic Linear Anisotropy Solving System (CLASS) II: Approximation schemes*, *JCAP* **07** (2011) 034 [1104.2933].
- [83] E.V. Linder and A. Jenkins, *Cosmic structure and dark energy*, *Mon. Not. Roy. Astron. Soc.* **346** (2003) 573 [astro-ph/0305286].
- [84] T. Brinckmann and J. Lesgourgues, *MontePython 3: Boosted MCMC sampler and other features*, *Physics of the Dark Universe* **24** (2019) 100260 [1804.07261].
- [85] B. Audren, J. Lesgourgues, K. Benabed and S. Prunet, *Conservative Constraints on Early Cosmology: an illustration of the Monte Python cosmological parameter inference code*, *JCAP* **02** (2013) 001 [1210.7183].
- [86] A. Lewis, *GetDist: a Python package for analysing Monte Carlo samples*, 1910.13970.
- [87] S. Nesseris and L. Perivolaropoulos, *Crossing the Phantom Divide: Theoretical Implications and Observational Status*, *JCAP* **01** (2007) 018 [astro-ph/0610092].
- [88] W. Hu, *Crossing the phantom divide: Dark energy internal degrees of freedom*, *Phys. Rev. D* **71** (2005) 047301 [astro-ph/0410680].
- [89] W. Fang, W. Hu and A. Lewis, *Crossing the Phantom Divide with Parameterized Post-Friedmann Dark Energy*, *Phys. Rev. D* **78** (2008) 087303 [0808.3125].
- [90] A.A. Costa, X.-D. Xu, B. Wang and E. Abdalla, *Constraints on interacting dark energy models from Planck 2015 and redshift-space distortion data*, *JCAP* **01** (2017) 028 [1605.04138].
- [91] S. Dodelson, *Modern Cosmology*, Academic Press, Amsterdam (2003).
- [92] DES collaboration, *Dark Energy Survey Year 3 results: Cosmology from cosmic shear and robustness to modeling uncertainty*, *Phys. Rev. D* **105** (2022) 023515 [2105.13544].
- [93] W. Hu, R. Barkana and A. Gruzinov, *Cold and fuzzy dark matter*, *Phys. Rev. Lett.* **85** (2000) 1158 [astro-ph/0003365].
- [94] M.-Y. Wang, A.H.G. Peter, L.E. Strigari, A.R. Zentner, B. Arant, S. Garrison-Kimmel et al., *Cosmological simulations of decaying dark matter: implications for small-scale structure of dark matter haloes*, *Mon. Not. Roy. Astron. Soc.* **445** (2014) 614 [1406.0527].
- [95] S.-H. Oh, C. Brook, F. Governato, E. Brinks, L. Mayer, W.J.G. de Blok et al., *The central slope of dark matter cores in dwarf galaxies: Simulations vs. THINGS*, *Astron. J.* **142** (2011) 24 [1011.2777].
- [96] W.J.G. de Blok and A. Bosma, *High-resolution rotation curves of low surface brightness galaxies*, *Astron. Astrophys.* **385** (2002) 816 [astro-ph/0201276].
- [97] B. Moore, S. Ghigna, F. Governato, G. Lake, T.R. Quinn, J. Stadel et al., *Dark matter substructure within galactic halos*, *Astrophys. J. Lett.* **524** (1999) L19 [astro-ph/9907411].
- [98] A.A. Klypin, A.V. Kravtsov, O. Valenzuela and F. Prada, *Where are the missing Galactic satellites?*, *Astrophys. J.* **522** (1999) 82 [astro-ph/9901240].
- [99] M. Boylan-Kolchin, J.S. Bullock and M. Kaplinghat, *Too big to fail? The puzzling darkness of massive Milky Way subhaloes*, *Mon. Not. Roy. Astron. Soc.* **415** (2011) L40 [1103.0007].
- [100] M. Boylan-Kolchin, J.S. Bullock and M. Kaplinghat, *The Milky Way's bright satellites as an apparent failure of LCDM*, *Mon. Not. Roy. Astron. Soc.* **422** (2012) 1203 [1111.2048].

- [101] A. Schneider, R.E. Smith and D. Reed, *Halo Mass Function and the Free Streaming Scale*, *Mon. Not. Roy. Astron. Soc.* **433** (2013) 1573 [[1303.0839](#)].
- [102] S. Bohr, J. Zavala, F.-Y. Cyr-Racine and M. Vogelsberger, *The halo mass function and inner structure of ETHOS haloes at high redshift*, *Mon. Not. Roy. Astron. Soc.* **506** (2021) 128 [[2101.08790](#)].
- [103] S. Pan, W. Yang, E. Di Valentino, D.F. Mota and J. Silk, *IWDM: the fate of an interacting non-cold dark matter — vacuum scenario*, *JCAP* **07** (2023) 064 [[2211.11047](#)].
- [104] P. Mukherjee and N. Banerjee, *Nonparametric reconstruction of interaction in the cosmic dark sector*, *Phys. Rev. D* **103** (2021) 123530 [[2105.09995](#)].
- [105] L.A. Escamilla, O. Akarsu, E. Di Valentino and J.A. Vazquez, *Model-independent reconstruction of the interacting dark energy kernel: Binned and Gaussian process*, *JCAP* **11** (2023) 051 [[2305.16290](#)].
- [106] A. Bonilla, S. Kumar, R.C. Nunes and S. Pan, *Reconstruction of the dark sectors' interaction: A model-independent inference and forecast from GW standard sirens*, *Mon. Not. Roy. Astron. Soc.* **512** (2022) 4231 [[2102.06149](#)].
- [107] Y. Kang, Y.-W. Lee, Y.-L. Kim, C. Chung and C.H. Ree, *Early-type Host Galaxies of Type Ia Supernovae. II. Evidence for Luminosity Evolution in Supernova Cosmology*, *Astrophys. J.* **889** (2020) 8 [[1912.04903](#)].